Journal of South American Earth Sciences 127 (2023) 104368

Contents lists available at ScienceDirect

Journal of South American Earth Sciences

journal homepage: www.elsevier.com/locate/jsames

Deciphering influencing processes in a tropical delta system (middle-late Eocene? to Early Miocene, Colombian Caribbean): Signals from a well-core integrative sedimentological, ichnological, and micropaleontological analysis

Sergio A. Celis [a,b,c,*], Francisco J. Rodríguez-Tovar [a,**], Andrés Pardo-Trujillo [b,c,d], Fernando García-García [a], Carlos A. Giraldo-Villegas [a,b,c], Fabián Gallego [b,c], Ángelo Plata [b,c,e], Raúl Trejos-Tamayo [b,c,e], Felipe Vallejo-Hincapié [b,c,e], Francisco Javier Cardona [f]

[a] Departamento de Estratigrafía y Paleontología, Universidad de Granada, 18002, Granada, Spain
[b] Instituto de Investigaciones en Estratigrafía-IIES, Universidad de Caldas, 170004, Manizales, Colombia
[c] Grupo de Investigación en Estratigrafía y Vulcanología (GIEV) Cumanday, Universidad de Caldas, Manizales, Colombia
[d] Departamento de Ciencias Geológicas, Universidad de Caldas, 170004, Manizales, Colombia
[e] Departamento de Geología, Universidad de Salamanca, 37008, Salamanca, Spain
[f] Consultant Geologist, Colombia

ARTICLE INFO

Keywords:
Fluvial/wave/tidal influence
Coarse-grained deltas
Hyperpycnal prodelta
Coal-bearing delta plain
Palynological analysis

ABSTRACT

Deltaic depositional systems are characterized by a complex interaction of physical, chemical, and biological factors. Although fluvial-, wave- and tidal-dominated deltaic environments have been extensively studied, evaluation of the processes in tropical mixed sedimentary systems has not been fully documented. Tropical regions with active margins are tectonic environments where these multiple factors act on the development of coastal systems. An onshore well-core from this tropical setting (Sinú-San Jacinto Basin, Colombian Caribbean) revealed that a middle-upper Eocene?-lower Oligocene coarse-grained deltaic setting is replaced by a thick coal-bearing mixed-energy fine-grained deltaic succession from the Oligocene to Early Miocene. The integrated analysis of facies associations, ichnological data, and terrestrial/marine micropaleontological assemblages (palynomorphs, foraminifera, and calcareous nannofossils) of this well-core allowed us to identify changes in dominance and influence of coastal processes (fluvial-, wave- and tide) and shoreline evolution. Using this information, as well as the sediment supply and accommodation space ratio, we were able to distinguish three intervals from the bottom to the top of the siliciclastic succession: (i) middle-late Eocene?–early Oligocene, prograding, fluvial-dominated, wave- and tide-influenced coarse-grained deltas with amalgamation of hyperpycnal-dominated mouth bars with hyperconcentrated flow input, (ii) Oligocene, retrograding to prograding, hyperpycnal-dominated heterolithic delta deposits punctuated by transgressive pulses, and (iii) late Oligocene to Early Miocene, aggradational, coal-bearing fine-grained delta plain with a higher proportion of transgressive phases over the continental environment. The complete succession represents long-term (~14 Myr) mixed-energy nearshore siliciclastic systems, showing different lithological arrangements and sedimentation styles. A long-term evolution is observed from a middle-late Eocene? steep, short and coarse-grained sedimentary system with tropical humid lowland forest and punctual development of macrobenthic tracemaker communities (Interval I) to an Early Miocene gently (poorly drained), well-developed delta plain with mangroves and wave- and storm-influence record through trace fossils assemblages (Interval III). A combination of factors, including subsidence, relief uplifting, and possible relative sea level changes, are interpreted as the main controls on the stratigraphic evolution of sedimentary styles throughout the entire succession. Minor-order sedimentary successions into each interval (e.g., prograding distributary mouth-bar channel) revealed short-term cycles presumably controlled by an internal delta dynamic. Multidisciplinary analysis is essential for recognizing the

* Corresponding author. Departamento de Estratigrafía y Paleontología, Universidad de Granada, 18002, Granada, Spain.
** Corresponding author. Departamento de Estratigrafía y Paleontología, Universidad de Granada, 18002, Granada, Spain.
E-mail addresses: sergio.celis@ucaldas.edu.co (S.A. Celis), fjrtovar@ugr.es (F.J. Rodríguez-Tovar).

https://doi.org/10.1016/j.jsames.2023.104368
Received 31 December 2022; Received in revised form 11 April 2023; Accepted 20 April 2023
Available online 26 April 2023

influence of fluvial, wave, and tidal processes on tropical deltas, where high spatial and temporal variability makes it difficult to determine dominant processes for long periods of time.

1. Introduction

The characterization of fluvial-, wave-, and tidal-dominated sedimentary successions in tropical regions has had broad attention in scientific and exploratory studies owing to the high sediment loads and their potential as reservoirs (e.g., Howell et al., 2008; Dalrymple et al., 2003; Shchepetkina et al., 2019, and references therein). The interplay of the fluvial, wave, and tidal processes over short spatial and temporal scales generates a high variability of marine mixed shoreline systems observed from modern environments and outcrops (Yang et al., 2005; Rossi and Steel, 2016). To highlight the great variability and complexity of ancient mixed-process shoreline systems, classifications that use qualitative descriptors (dominated-, influenced-, affected-) of fluvial, wave, and tidal processes have often been used to characterize sedimentary deposits (Ainsworth et al., 2011). Alternative ways of characterizing the internal facies complexity include methods that quantify the likelihood that a deposit was formed by wave, tide, or fluvial processes on the basis of dominant sedimentary structures, texture, and bioturbation. This is especially useful in core data where 3D features of the sedimentary bodies (e.g., bed geometry) are difficult to observe (MacEachern et al., 2005; Bhattacharya, 2006; Wei et al., 2016; Rossi et al., 2017).

Nonetheless, although specific sedimentary environments within coastal successions have characteristic facies associations, their

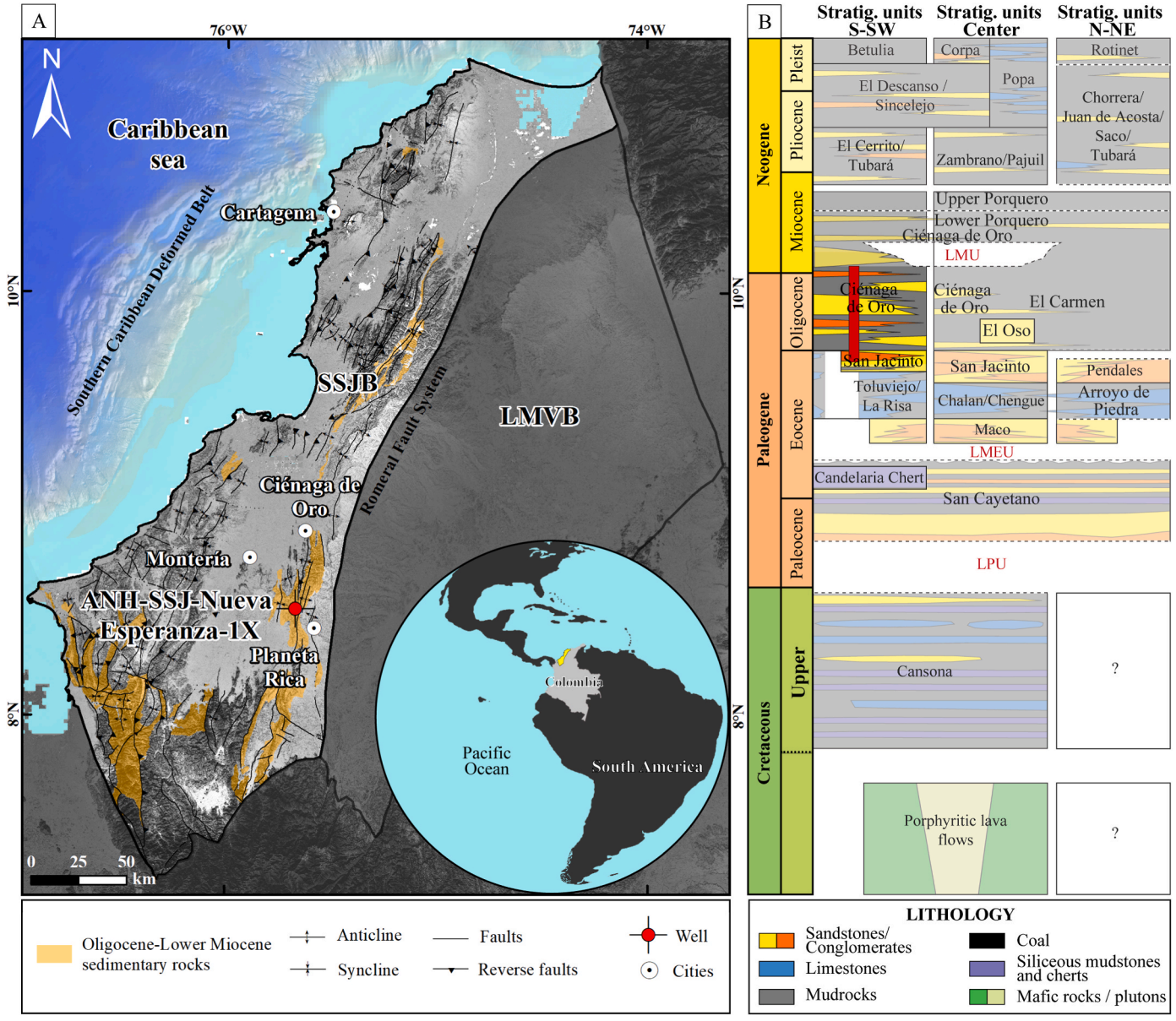

Fig. 1. A. Location of Colombia in South America (yellow polygon for the SSJB) and location of the SSJB in the Colombian Caribbean. Only Oligocene-Lower Miocene deposits are indicated in the SSJB (Source: WGS-1984 coordinate system; CIOH, SRTM, NOAA elevation, and ocean models; geology from Gómez et al., 2015). **B.** Schematic chronostratigraphic chart of the SJFB (modified from Mora et al., 2017, 2018; Osorio-Granada et al., 2020). LPU: lower Paleocene unconformity; LMEU: lower-middle Eocene unconformity; LMU: lower Miocene unconformity. Red bar: cored section.

recognition should not be based only on physical structures; under certain depositional conditions, they can appear similar depending on the interactions of various parameters (MacEachern et al., 2005; Bhattacharya, 2006; Dalrymple and Choi, 2007; Ainsworth et al., 2011). For this reason, ichnological and micropaleontological analyses integrated into the detailed sedimentological description have become fundamental tools for interpreting such settings (Nagy, 1992; MacEachern et al., 2005; Gani et al., 2007; MacEachern and Bann, 2008, 2020; Slater et al., 2017; Chalabe et al., 2022), although studies integrating all three tools are scarce (e.g., MacEachern et al., 1999).

Ichnology is useful for paleoenvironmental interpretation because of the extreme sensitivity of tracemakers—their behavior, hence the generated structures—to specific environmental conditions (MacEachern et al., 2005; MacEachern and Bann, 2008). Although depositional systems are widely studied, a sound understanding of organism responses to the interplay of processes and environmental conditions operating in coastal depositional settings is still being developed (MacEachern and Bann, 2020 and references therein).

In addition to ichnology, the characterization of organic matter is key to deciphering the fluvial signal in mixed-energy coastal systems (Zavala et al., 2012). Macroscopic and microscopic vegetal remains (e.g., coal, wood fragments, leaves, pollen, and spores) are abundant components of fluvial-dominated deposits accumulated at the river mouth during flooding events (Slater et al., 2017). Anaysis of palynomorphs, which are well preserved in hyperpycnal-dominated subaqueous delta subenvironments (e.g., prodelta), is important for reconstructing subaerial deltaic subenvironments (e.g., feeder system, upper delta plain, interdistributary bays). This information is highly useful in tropical or subtropical settings where coastal systems represent reservoirs of organic matter (Hoorn, 1994; Birgenheier et al., 2017).

Here we apply a multidisciplinary approach to a study of a ~700 m-thick middle-late Eocene? to Early Miocene well-core in a tropical basin (Colombian Caribbean onshore region, Fig. 1), to reconstruct dominant processes of sedimentation and depositional environments evolution in mixed-energy coastal systems. The Oligocene-Miocene coastal systems of the Colombian Caribbean have been extensively studied because some of their deposits are proven hydrocarbon reservoirs (Flinch, 2003). Nonetheless, published data from sedimentological, ichnological and micropaleontological studies for detailed paleoenvironmental purposes of this time interval are still in their early stages. Accordingly, the objectives of this paper are: (a) to document tracemaker-substrate interactions to establish the paleoenvironmental (depositional and ecological) variations in the coastal systems occurred from the middle-late Eocene? to Early Miocene in the Colombian Caribbean; and (b) to discuss paleogeographical implications supported by previous regional models.

2. Geological setting

The ongoing interaction of the Caribbean Plate against the NW margin of South America has influenced the sedimentation of the Colombian Caribbean basins since the Cretaceous (Montes et al., 2019; Mora-Páez et al., 2019; Romito and Mann, 2020). GPS and seismic data have shown that coeval oblique convergence of NW South America and the Caribbean from the Upper Cretaceous to the lower Eocene, nearly orthogonally convergence from the Oligocene until today (Mora-Bohórquez et al., 2020 and references contained herein). The Sinú-San Jacinto Basin (SSJB) of northern Colombia (Fig. 1A) is considered a forearc basin with an oceanic igneous basement of Cretaceous age (Geotec, 2003; Guzmán, 2007; Bermúdez et al., 2009; Silva-Arias et al., 2016; Mora et al., 2017). Its sedimentary fill includes rocks from the Upper Cretaceous to Pleistocene with several unconformities and variations in accommodation space linked to the multi-stage tectonic interaction of the Caribbean and South American plates (Mantilla-Pimiento et al., 2009; Noda, 2016; Mora et al., 2017, 2018; Montes et al., 2019; Pardo-Trujillo et al., 2020). Tectonic evolution of the Colombian Caribbean has generated a folded belt with a current SW-NE direction, which exposes the Upper Cretaceous to the Pliocene-Pleistocene rocks of the basin at the surface in what is now referred to as the San Jacinto Fold Belt (SJFB; Fig. 1A).

The ANH-SSJ-Nueva Esperanza-1X stratigraphic well-core drilled deposits in the San Jacinto Fold Belt associated with the Ciénaga de Oro Formation (COF) (Gómez et al., 2015) and possibly with the San Jacinto Formation, owing to interest as hydrocarbon reservoirs (Fig. 1B) (Flinch, 2003). Even though the tectonic evolution of the continental margin and its relationship with sedimentary environments is still a matter of debate, there is a consensus that the COF was deposited in shallow marine and deltaic systems with dominant fluvial processes favoring the development of mangrove areas and accumulations of coal beds in the SW Colombian Caribbean (Dueñas and Duque-Caro, 1981; Dueñas, 1983, 1986; Guzmán et al., 2004; Bermúdez et al., 2009; Bermúdez, 2016; Manco-Garcés et al., 2020; Celis et al., 2021). Dueñas (1980, 1983, 1986) and Guzmán et al. (2004) assigned a late Eocene to Early Miocene age to the COF based on palynological and foraminiferal biostratigraphic studies. Dueñas (1983) concluded that the coastal mangrove areas during the Oligocene were affected by sea-level variations. Their carbonaceous content could correlate with the Amagá Formation outcropping in the Amagá sub-basin in the Cauca depression in central Colombia.

The stratigraphic relationship of the COF to the overlying and underlying units in the south-southwest of the SJFB is not yet clearly established. In this part of the basin, rocks of this unit crop out in unconformable contact on rocks possibly associated with the Paleocene-Eocene San Cayetano Formation (Dueñas and Duque-Caro, 1981; Dueñas, 1983, 1986; Mora et al., 2017). However, based on the compilation of unpublished information from the hydrocarbon industry, some outcrop studies from the central and central-northeastern regions of the SJFB (Guzmán et al., 2004; Raigosa, 2018; SGC, 2019; Salazar-Ortiz et al., 2020), and the results obtained in this work, we suggest that in the southern part of the basin there are two formations underlying the COF in addition to the San Cayetano Formation (Fig. 1B): the San Jacinto Formation consisting of conglomerates, sandstones, and sandy siltstones of late Eocene to early Oligocene age (Duque-Caro, 1972; Duque-Caro et al., 1996; SGC, 2019), and the Toluviejo Formation with bioclastic limestones from the upper Eocene (Guzmán et al., 2004; Raigosa, 2018). Mora et al. (2018), using seismic data, suggested that an Early to Middle Miocene unconformity (LMU) divides the COF. However, in some sectors of the basin, this unconformity has not been identified. The COF is overlain by marine siltstones and, in a lesser proportion, sandstones corresponding to the Porquera Formation accumulated during the Early-Middle to Late Miocene (Guzmán, 2007; Mora et al., 2017).

3. Materials and methods

The studied cored section corresponds to the ANH-SSJ-Nueva Esperanza-1X stratigraphic well (~691 m in thickness) drilled in the south-western zone of the SJFB (Fig. 1). The new specific data and the well-established chronostratigraphic framework presented in this study have made it possible to specify the depositional models based on an earlier study that was published in this journal (Celis et al., 2021). Detailed logging (scale 1:5) considered the lithology (texture: grain size, sorting, roundness, sphericity), bed thickness and contact types, fossil content, and sedimentary structures (physical, biogenic, and chemical). Mudrocks refer to rocks with grain size <1/16 mm, and claystones to those where the <1/256 mm fraction was recognized (Wentworth, 1922). For textural and compositional information about mixed rocks, we followed the proposal of Mount (1985), modifying the allochemic term to bioclastic, because the mixed rocks often consist of fragments of broken shells and extraclasts. Additionally, the conglomerate grain-size was included in this nomenclature. In that sense, the terms conglomerate, sandstone, or mudrock refer to the grain-size of the terrigenous

portion, and the term bioclastic refers to the bioclastic material independent of the grain-size of the bioclasts. Facies codes were assigned following Reading (1996) and Collinson and Mountney (2019), based on lithology and sedimentary structures.

Bed thickness was classified as very thin (<1 cm), thin (1–10 cm), medium (11–30 cm), thick (31–100 cm), and very thick (>100 cm) (Nichols, 2009 and references therein). Detailed ichnological analyses were conducted, including major ichnological attributes such as ichnodiversity, distribution, abundance (Bioturbation Index BI *sensu* Taylor and Goldring, 1993) of the structures and their relationship with the facies and stratigraphic surfaces. We used an ichnological atlas on core images (Frey and Pemberton, 1985; Gerard and Bromley, 2008; Knaust, 2017) to make ichnotaxonomic assignments of trace fossils based on the overall shape and the presence of specific diagnostic criteria or ichnotaxobases (Bromley, 1996; Bertling et al., 2006). Due to core limitations, ichnotaxonomic classification was made to the ichnogenus level (Bromley, 1996). Although the well-core was not slabbed, only ichnotaxa that could be confidently identified by ichnotaxonomic features were considered in the analysis. Those that posed any doubts were marked with a question mark and used with caution in the interpretations.

To undertake a detailed analysis of a complex environment, such as coastal settings, in which different processes are interrelated (e.g., fluvial, tidal, and waves), we follow the nomenclature used by MacEachern et al. (2005) and Bhattacharya (2006) for paleoenvironmental zonation. Sampling was carried out in mudrocks lithologies. Micropaleontological analyses (of palynomorphs, foraminifera, calcareous nannoplankton) were conducted for biostratigraphic and paleoenvironmental purposes. A total of 72 palynological samples were treated using the standard technique described by Traverse (2007). Slides were scanned using a high-resolution Nikon Eclipse 80i microscope at 40x and 100× magnification. Abundance of each sample was estimated by counting palynomorphs up to 300 specimens as far as possible and then assigned to the following categories: 1) barren: no palynomorphs recorded; 2) moderate to scarce: 1–200 palynomorphs; and 3) abundant: >200 palynomorphs. The palynological age model relied on the Cenozoic zonation of Jaramillo et al. (2011). The palynomorphs were grouped by botanical affinities and ecological significance, with the sum of the groups totaling 100%. The ecological assignments were based on Hoorn (1994), Jaramillo et al. (2010), Pardo-Trujillo and Jaramillo (2014), and D'Apolito et al. (2021). Thermal maturation estimations were made using Pearson's (1984) color chart correlated with corresponding Thermal Alteration Index (TAI) values, as illustrated in Traverse (2007).

The preparation of 71 foraminiferal samples follows the methodology of Thomas and Murney (1985). Samples were wet-washed using a 63 μm and 125 μm mesh sieve. This fraction was analyzed under a high-resolution Nikon PET SMZ1500 optical stereomicroscope. The photographs were taken using the ESEM-Quanta 250 and the mini-sputtering technique. Abundances, based on the total of foraminifera per gram of sediment (f/g), were categorized as very abundant (VA): >150 f/g, abundant (A): 70–150 f/g, common (C): 30–70 f/g, rare (R): 1–30 f/g, and barren (B): no recovery. Preservation was defined in terms of poor, moderate, and good. Taxonomic criteria follow Wade et al. (2018), and planktonic foraminiferal zonation follows Wade et al. (2011). Seventy-one calcareous nannofossil slides were prepared after applying the smear slide technique, then analyzed under a petrographic microscope Nikon Eclipse LV100 optical microscope at 1000x coupled with a high-resolution Nikon DS-F11 camera. Calcareous nannofossils were quantified by counting up to 500 specimens per sample or, in cases of very rare nannofossils, up to a total of 500 fields of view. Preservation was qualitatively evaluated as follows: poor (1): recrystallized and/or dissolved specimens, preventing taxonomic classification; moderate (2): slight dissolution and/or recrystallization that does not preclude species identification, although some diagnostic characteristics have been affected; and good (3): little evidence of dissolution and/or regrowth, the morphology of the specimen is clear. Classification of calcareous nannofossils was based on usual taxonomic concepts and catalogues (Perch-Nielsen, 1985; Bown, 1998; Young et al., 2003, 2017; Aubry, 2014a, 2014b, 2015b, 2015a, 2021). Biostratigraphic information of this group followed the biozonation of Martini (1971). Chronostratigraphic assignments relied on the International Chronostratigraphic Chart (Cohen et al., 2013) and nomenclature formally established by the Subcomissions of the International Commission on Stratigraphy (https://stratigraphy.org/subcommissions).

4. Results

4.1. Biostratigraphy

Biostratigraphy in the ANH-SSJ-Nueva Esperanza-1X core section is based on palynomorphs, planktonic foraminifera, and calcareous nannofossils (Figs. 2 and 3). The preservation of palynomorphs is moderate to good, and the abundance ranges from low to very abundant. The thermal alteration index based on the color of spores suggests immature rocks (TAI: 2 to 2+). Planktonic foraminifera and calcareous nannofossils are scarce and poorly to moderately preserved. Benthic foraminifera are nearly absent and poorly preserved, and, therefore, they could not be recognized even at the genus level and were not used as palaeoenvironmental indicators.

According to the stratigraphic distribution, microfossil abundance patterns, and the presence of some key taxa, the cored section can be divided into three intervals, from base to top (Figs. 2 and 3). Interval 1 at the base of the core (~690 m–~625 m) is characterized by the exclusive recovery of palynomorphs that include *Perisyncolporites pokornyi* and *Polypodiisporites usmensis*. The assemblage indicates an age younger than or equal to the middle Eocene, and constraints the top of interval 1 to younger than or equal to the late Eocene (Figs. 2 and 3), T06 to T07 zones of Jaramillo et al. (2011). No marine microfossils were found.

Interval 2 (~623–~164 m) is characterized by a palynological assemblage consisting of *Bombacacidites echinatus*, *Cicatricosisporites dorogensis*, *Crassiectoapertites columbianus*, *Magnaperiporites spinosus*, *Magnastriatites grandiosus*, *Psilatricolporites pachydermatus*, *Rhoipites planipolaris* and *Spinizonocolpites echinatus*, indicating a biozonal range from T08 to T11, restricted to the Oligocene (Jaramillo et al., 2011). Planktonic foraminifera identified at ~533 m consist of *Catapsydrax unicavus*, *Ciperoella anguliofficinalis*, *C. angulisuturalis*, *C. ciperoensis*, *Globorotaloides hexagonus*, *G. variabilis*, *Globoturborotalita bassriverensis*, *G. gnaucki*, *G. ouachitaensis*, *G. pseudopraebulloides*, *G. woodi*, *Tenuitella angustiumbilicata*, *Turborotalita praequinqueloba*, *Paragloborotalia nana*, and *Subbotina eocaena.* These taxa coexisted in biozone O4 of Wade et al. (2011) from the younger part of the early Oligocene. Calcareous nannofossils consist of abundant *Cyclicargolithus abisectus*, *Cyclicargolithus floridanus*, *Coccolithus pelagicus*, *Discoaster deflandrei*, *Reticulofenestra* spp., and *Sphenolithus* spp., and sporadic *Reticulofenestra bisecta*. Among them, *C. abisectus*, observed from ~526 to ~433 m, indicates a biozonal interval from NP23 to NN1 (Martini, 1971) whose age range is from Oligocene to the earliest Miocene (Perch-Nielsen, 1985; Backman et al., 2012; Agnini et al., 2014). Although *R. bisecta* was observed only at ~526 m, this species became extinct in the late Oligocene (Perch-Nielsen, 1985; Backman et al., 2012; Agnini et al., 2014), supporting a Paleogene age for this interval. These considerations of interval 2 indicate that interval 1 is neither older than middle-late Eocene? Nor younger than early Oligocene age.

Interval 3 from ~164 m to ~5 m, yielded the palynomorphs *Bombacacidites gonzalezii*, *Bombacacidites muinaneorum*, *Cyclusphaera scabrata*, *Nijssenosporites fossulatus*, and *Proteacidites triangulatus* indicating the Early Miocene (T12 palynologic zone). The occurrence of *Bombacacidites echinatus*, *Cicatricosisporites dorogensis*, and *Spinizonocolpites echinatus*, is interpreted as a consequence of reworking from Paleogene beds. Toward the top of the well-core (~15 m–~18 m), planktonic foraminifera *Paragloborotalia continuosa*, *Tenuitella angustiumbilicata*,

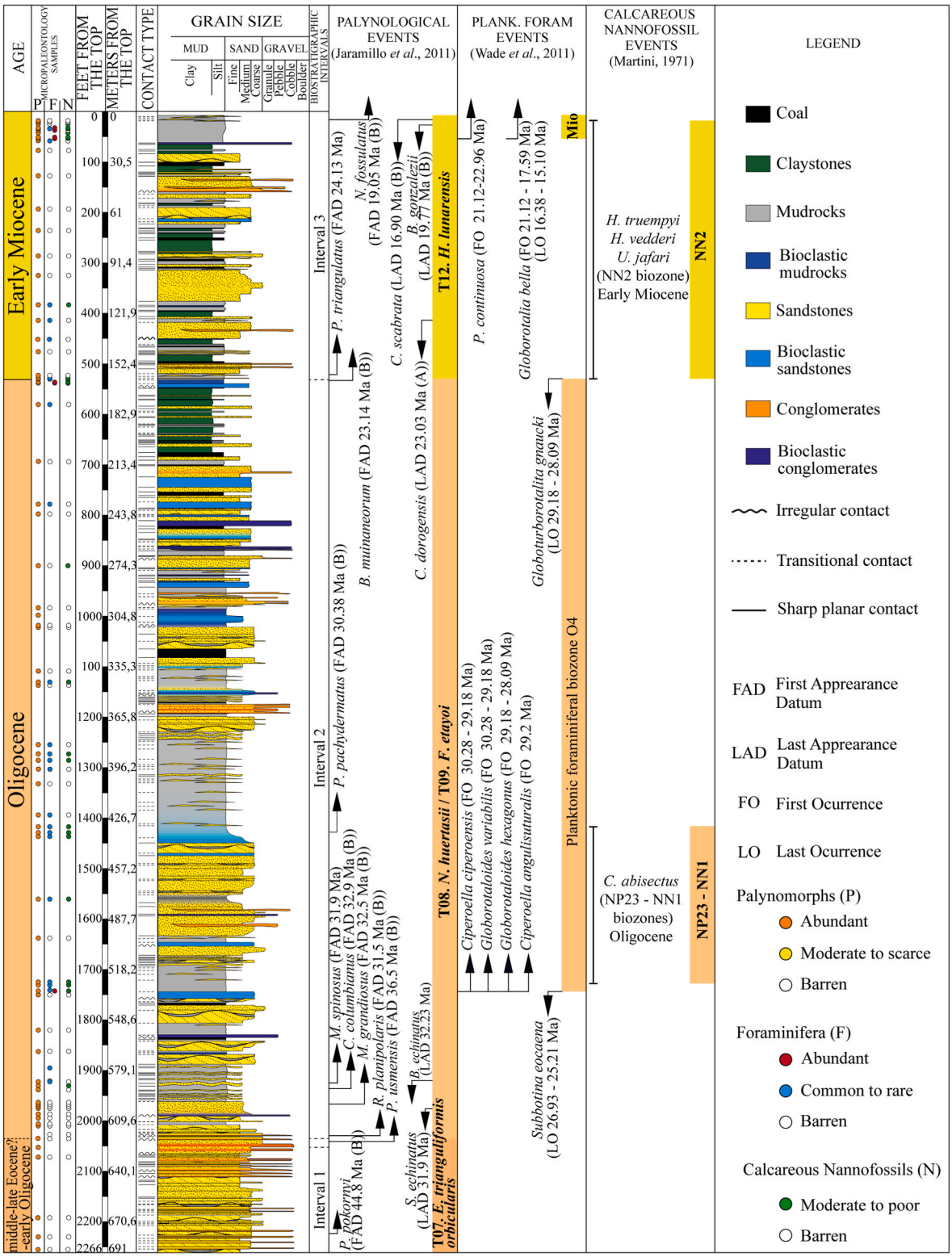

Fig. 2. Age, biostratigraphic samples distribution, stratigraphic log, and bioevents found in the ANH-SSJ-Nueva Esperanza-1X stratigraphic well.

Globoturborotalita woodi, *G. pseudopraebulloides*, *G. ouachitaensis*, *G. gnaucki, Globorotalia bella,* and *Globigerina bulloides* indicate M1b-M5 biozones, spanning the Early to Middle Miocene (Figs. 2 and 3). The occurrence of *G. gnaucki* reveals reworking from the lower Oligocene beds. New taxa of calcareous nannofossils such as *Helicosphaera euphratis, H. vedderi, H. truempyi, Umbilicosphaera jafari,* and *Sphenolithus conicus* are registered. The occurrence of *H. vedderi* and *H. truempyi*, between 164 m and ~8 m, indicates biozone NN2 (Young, 1998; Boesiger et al., 2017), supporting an Early Miocene age. Moreover, calcareous nannofossil taxa similar to those of the previous interval are recorded, providing evidence of reworking of Oligocene marine deposits in the third interval.

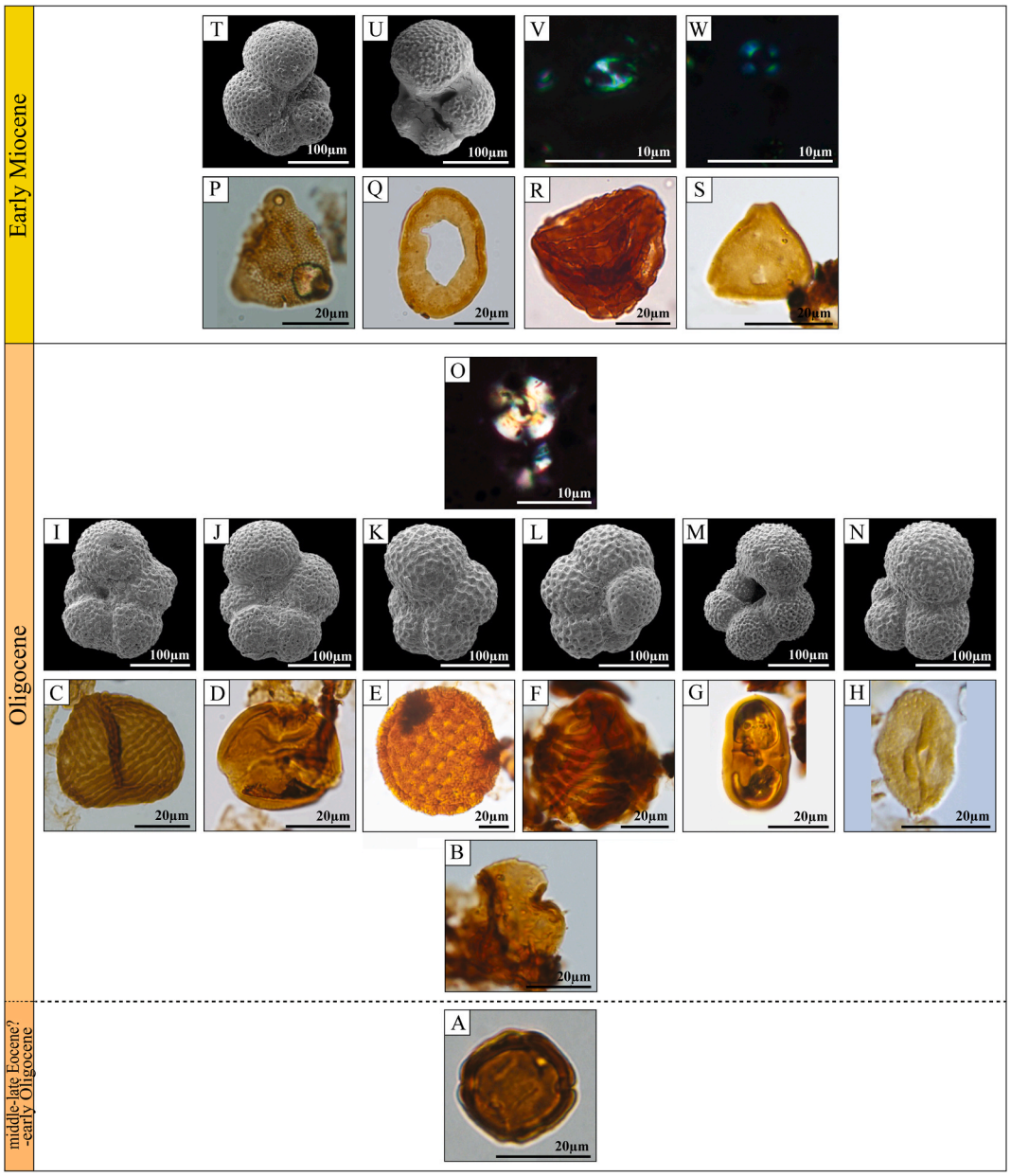

Fig. 3. Some micropaleontological key taxa**. Interval 1. Palynomorphs: A.** *Perisyncolporites pokornyi*. **Interval 2. Palynomorphs: B.** *Bombacacidites echinatus*. **C.** *Cicatricosisporites dorogensis*. **D.** *Crassiectoapertites columbianus*. **E.** *Magnaperiporites spinosus*. **F.** *Magnastriatites grandiosus*. **G.** *Psilatricolporites pachydermatus*. **H.** *Rhoipites planipolaris*. **Foraminifera: I.** *Ciperoella angulisuturalis*. **J.** *C. ciperoensis*. **K.** *Globorotaloides hexagonus*. **L.** *G. variabilis*. **M.** *Globoturborotalita gnaucki*. **N.** *Subbotina eocaena*. **Calcareous nannofossil: O.** *Cyclicargolithus abisectus*. **Interval 3. Palynomorphs: P.** *B. muinaneorum*. **Q.** *Cyclusphaera scabrata*. **R.** *Nijssenosporites fossulatus*. **S.** *Proteacidites triangulatus*. **Foraminifera: T.** *Globorotalia bella*. **U.** *Paragloborotalia continuosa*. **Calcareous nannofossil: V.** *Helicosphaera vedderi*. **W.** *Umbilicosphaera jafari*.

4.2. Palynomorph groups with ecological significance

The groups of palynomorphs observed were classified according to their taxonomic affinities: pteridophyte spores, undifferentiated angiosperm pollen, lowland forest, palmae, morichal palmae, mangroves, fungal remnants, and marine palynomorphs (Fig. 4; Appendix 1). In general, the palynological record indicates humid tropical lowland forests. High concentrations of fungal remnants suggest high humidity, and the common record of moriche palms points to typical flooded zones along riverbanks. Mangrove pollen indicate areas near the coast. Marine palynomorphs can be useful for identifying relative variations in the sea level.

Interval I, the lower portion of the section (between ~690 m and ~625 m) is characterized by abundant pollen and spores (~25%–~30% on average), some of them of lowland forests (~10%–~50%) (Fig. 4; Appendix 1). In addition, fungal remains (~10%) are identified (Fig. 4; Appendix 1). Local variation in abundance is significant, however; the lowland forest component varies from 10% to ~50% and abundance of fungal remnants varies from ~10% to ~53%

In Interval 2 (from ~614 m), we found a decrease in pollen and spores (~20%–~25% on average) and abundances of lowland forest similar to those in the previous interval (~25%). Local increases in fungal remnants of up to 50% are seen mainly in this interval (~50%) (Fig. 4). Palynomorphs of palmae show very low recovery in the section (~1% on average). Instead, morichal palm forest becomes evident —an ecological group that varies only slightly throughout the studied section (~10% on average), although it shows a slight increase in the middle-upper part (~15% on average) (from ~350 to ~91 m) (Fig. 4;

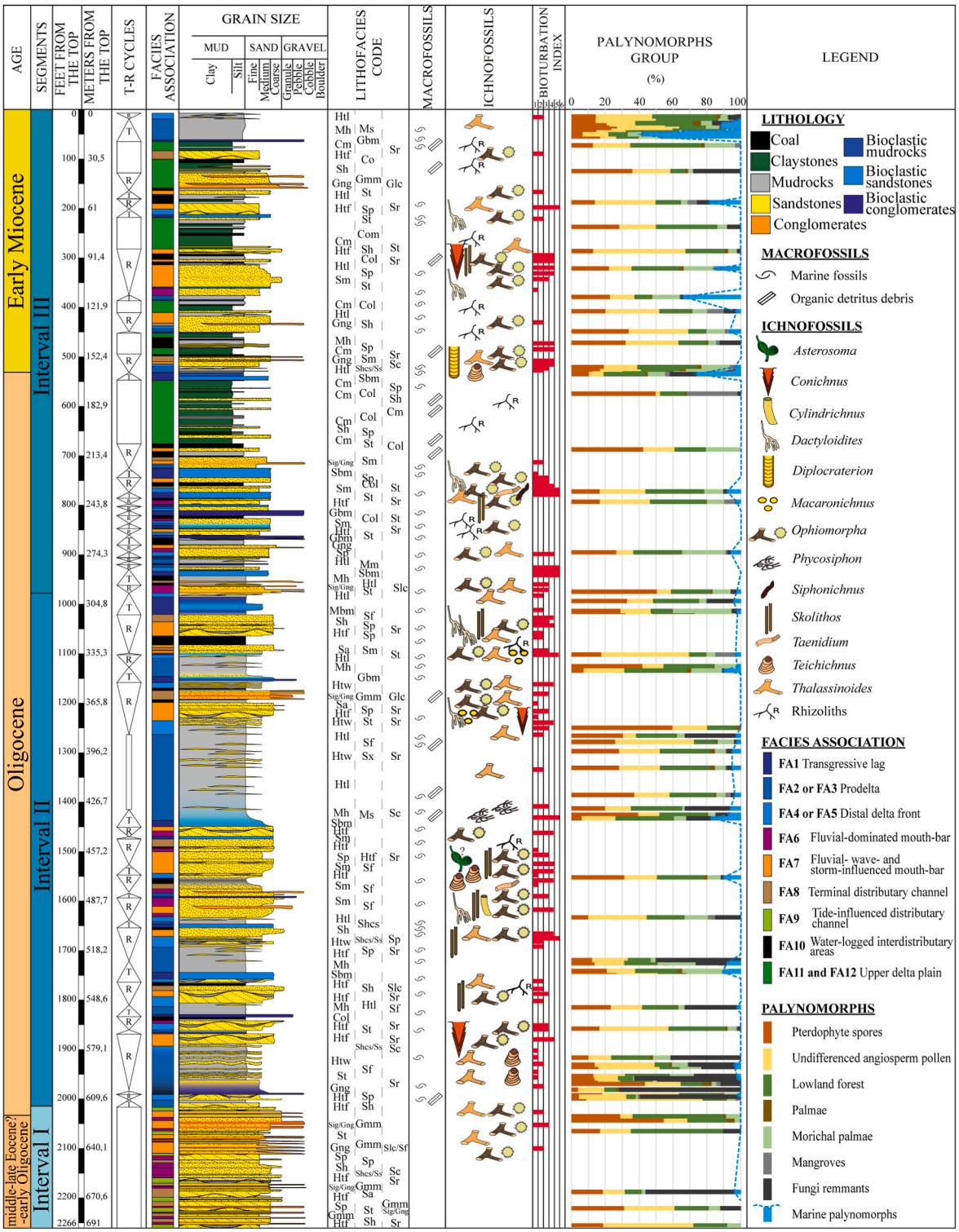

Fig. 4. Stratigraphic log of the cored section (scale 1:2000), including Transgressive-Regressive cycles (T-R cycles), sedimentological (lithology, sedimentary structures, and facies associations), and paleontological features (macrofossils, ichnofossils, Bioturbation Index, and palynomorph groups). Table 1 provides detailed information about the facies code.

Appendix 1).

Interval three sees a gradual increase in marine palynomorphs such as dinoflagellate cysts and foraminiferal organic linings (~2% on average, and an increase to ~11% at the top; from ~164 m) (Fig. 4; Appendix 1). Similarly, an increase in *Zonocostites* and *Lanagiopollis crassa*, which are associated with mangrove ecosystems, is observed at ~176 m (~30%). However, mangrove palynomorphs are particularly rare along the entire record (~1% on average). The average abundance of spores, pollen, and lowland forest is maintained.

4.3. Facies associations analysis

Twenty-eight sedimentary facies were defined throughout the ANH-SSJ-Nueva Esperanza-1X stratigraphic cored section (Table 1) (see Celis

Table 1
Sedimentary facies identified in the ANH-SSJ-Nueva Esperanza-1X well-core.

Facies Code	Lithology and sedimentary structures	Components and texture (Note: also include microfossil content)	Ichnology	Bed/set thickness (cm)
Gmm	Massive matrix-supported massive conglomerates	- Matrix: fine- to medium-grained sandstone. - Clasts: granule-size and a lesser extent, pebble-size. Quartz; feldspars in less proportion; metamorphic lithic occasionally. Sub-rounded to rounded and low sphericity. - Moderately to poorly sorted; occasionally well sorted.	BI = 0–3; *Ophiomorpha*.	5–150
Gcm	Massive clast-supported massive conglomerates	- Clasts: granule-size and a lesser extent, pebble-size. Quartz; feldspars in less proportion. Sub-rounded to rounded and low sphericity. - Moderately to poorly sorted. - Matrix: fine-grained sandstone.		5–20
Gng	Normally graded, matrix-supported conglomerates to sandstones	- Matrix: fine-grained sandstone. - Conglomerates: granule-sized and a lesser extent, pebble-sized clasts. Quartz; feldspars in less proportion. Sub-rounded to rounded and high sphericity. Moderately sorted. To - Sandstones: coarse- to medium-grained, mainly quartz.	BI = 0–3; *Ophiomorpha*.	5–80
Sig	Inversely graded sandstones, conglomeratic sandstone to matrix-supported conglomerates	- Sandstones: coarse- to medium-grained, mainly quartz. To - Matrix: fine-grained sandstone. - Conglomerates: granule-sized and a lesser extent, pebble-sized clasts. Quartz and feldspars. Sub-rounded to rounded and high sphericity. Moderately to poorly sorted.		5–60
Sng	Normally graded sandstones	Medium- to coarse-grained to fine and very fine-grained. Quartz; feldspars in less proportion. Moderately to poor sorted.	BI = 0–3; *Ophiomorpha*.	5–60
Sm	Massive sandstones	Fine- to coarse-grained. Quartz; feldspars and metamorphic lithics in less proportion. Moderately to well sorted.	BI = 0–6; *Dactyloidites*, *Macaronichnus*, *Ophiomorpha, Siphonichnus.*	5–200
Sh	Horizontal laminated sandstones	Fine- to medium-grained. Quartz; feldspars in less proportion. Well sorted.	BI = 0–4; *Conichnus*, *Cylindrichnus*, *Dactyloidites*, *Macaronichnus*, *Ophiomorpha*, *Skolithos*, *Thalassinoides*, rhizoliths.	5–60
Sa	Low-angle cross-bedded sandstones	Fine- to medium-grained. Quartz; feldspars in less proportion. Well sorted.	BI = 0–3; *Dactyloidites*, *Ophiomorpha*.	5–30
Sp	Planar cross-bedded sandstones	Fine- to medium-coarse-grained Quartz; feldspars in less proportion. Moderately to well sorted.	BI = 0–3; *Ophiomorpha*, *Skolithos.*	5–60
St	Trough cross-bedded sandstones	Fine- to medium-grained Quartz; feldspars in less proportion. Moderately to well sorted.	BI = 0–2; *Ophiomorpha*.	5–30
Sr	Sandstones with asymmetric ripple cross-lamination	Fine- to medium-grained. Quartz; feldspars in less proportion. Moderately to well sorted.	BI = 0–1; *Teichichnus*.	<5
Sw	Sandstones with symmetric ripple cross-lamination	Fine- to medium-grained. Quartz; feldspars in less proportion. Well sorted.	BI = 0–2; *Teichichnus*.	<5
Sc	Sandstones with soft-sediment deformation structure	Fine- to medium-grained. Quartz; feldspars in less proportion. Moderately to poor sorted.		5–30
Shcs	Sandstones with hummocky cross-stratification	Fine- to medium-grained. Quartz; feldspars in less proportion. Well sorted.		2–10
Ss	Sandstones with swaley cross-stratification	Fine- to medium-grained. Quartz; feldspars in less proportion. Well sorted		2–10
Htf	Heterolithic mudstone-sandstone alternation with flaser bedding	- Sandstones: Fine-grained, and occasionally medium- to coarse-grained. Quartz	BI = 0–4; *Conichnus*, *Cylindrichnus*, *Dactyloidites*, *Macaronichnus*,	5–60

(*continued on next page*)

Table 1 (*continued*)

Facies Code	Lithology and sedimentary structures	Components and texture (Note: also include microfossil content)	Ichnology	Bed/set thickness (cm)
		and feldspars. Moderately to well sorted.	*Ophiomorpha*, *Skolithos*, *Thalassinoides*, rhizoliths.	
Htw	Heterolithic mudstone-sandstone alternation with wavy bedding	- Sandstones: Fine-grained. Quartz and feldspars. Moderately to well sorted.	BI = 0–2; *Skolithos* and *Ophimoprha.*	5–30
Htl	Heterolithic mudstone-sandstone alternation with lenticular bedding	- Sandstones: Fine-grained. Quartz and feldspars. Moderately sorted.	BI = 0–2; *Taenidium*, *Teichichnus*.	5–3000
Slc, Sf	Load casts and flame structures in sandstones, conglomerates, and mudrocks	Occur at the bases of Gmm, Gcm, Gng, Sm, Sh, Mm.		<5
Mm	Massive mudrocks		BI = 0–6; *Phycosiphon*, rhizoliths.	5–300
Mh	Horizontal laminated mudrocks		BI = 0–2; *Teichichnus*.	5–500
Ms	Mudrocks with syneresis cracks			<5
Cm	Claystones		BI = 0–1; rhizoliths.	5–150
Col	Laminated coal		BI = 0–3; *Thalassinoides*.	10–100
Com	Structureless coal			10–20
Gbm	Massive bioclastic conglomerates	- Terrigenous grains: granule size, quartz. Poor sorted. - Bioclastic grains: granule- and pebble size, bivalves and gastropod, moderately sorted. - Matrix: fine- to medium-grained. Quartz, feldspars, and micrite.	BI = 0–2; *Ophiomorpha*.	10–200
Sbm	Massive bioclastic sandstones	- Terrigenous grains: fine- to medium-grained, quartz, moderately sorted. - Bioclastic grains: granule-sized, bivalves and gastropods, moderately to poorly sorted.	BI = 0–3; *Ophiomorpha*.	10–300
Mbm	Bioclastic mudrocks	- Bioclastic grains: granule-sized, bivalves and gastropods, moderately to poorly sorted.	BI = 0–3; *Ophiomorpha*.	10–300

et al., 2021 for a previous detailed study of some of them). The recognized lithofacies have been grouped into 12 facies associations (FA; Table 2) described below (Table 3).

4.3.1. Facies association 1 (FA1)

Description: FA1 presents thick beds up to 8 m thick (commonly 3–4 m thickness) of structureless bioclastic deposits (bioclastic sandstones, Sbm; bioclastic conglomerates, Gbm; bioclastic mudrocks, Mbm). Allochemical components are represented by fossils (bivalves, gastropods [*Aclis* spp., *Turritella* spp.], scaphopod fragments, indeterminate shells and shell hash), which are frequently randomly distributed, and in lesser proportion by muddy intraclasts (Fig. 5A and B; Table 3). The contact with the underlying bed (coal or mudrocks) is irregular and bioturbated by *Thalassinoides* (BI = 0–3). Occasionally and transitionally to the top, these lithologies present a decrease in shells and are bioturbated by *Ophiomorpha* in the upper part of the bioclastic deposits (e.g., ~223 m). To the top, FA1 exhibits transitional variation to FA2 (fluvial-dominated prodelta) or FA3 (mixed prodelta).

4.3.1.1. Interpretation: transgressive lag. The bases of these deposits are irregular, over coal and mudrock beds (FA10), reflecting an erosive process. Bioclastic sediments (Sbm, Gbm, Mbm) and shell hash distributed randomly (FA1) suggest rapid transgressive pulses, or storms (Savrda et al., 1993; Schultz et al., 2020). The bases are invariably bioturbated by *Thalassinoides* in coal and mudrock beds, which could be attributed to bioturbation in a firmground associated with *Glossifungites* ichnofacies (Pemberton et al., 1992, 2004; MacEachern et al., 2007a, 2007b). The decrease in the accumulation of random shells and softground bioturbation represented by *Ophiomorpha* suggest colonization of the substrate during a period of decreasing energy towards the top of the bioclastic deposits, allowing the establishment of a macrobenthic community. This FA represents a transition to deeper-water deposits, during delta-lobe abandonment, drowning of the river-dominated delta plain, or a wave-dominated strandplain (Cattaneo and Steel, 2003; Buatois et al., 2012).

4.3.2. Facies association 2 (FA2)

Description: FA2 presents thick beds (31–100 cm) resulting in succesions up to 45 m thick of mudrocks and sandy mudrocks, structureless (Mm) or with horizontal lamination (Mh); it has a low bioturbation index (BI = 0–1) and is associated with *Planolites* and locally exclusive and abundant *Phycosiphon* (BI = 4–5; Fig. 5C and D). Further, we recovered some calcareous nannofossils and foraminifera (Table 3). Occasionally, there are very fine-grained sandy mudrocks with normal grading to mudrocks (Sng), as well as palynomorphs (Fig. 5C; Table 3). These deposits vary transitionally to intercalations of thick beds of mudrocks and very fine-to fine-grained sandstones with horizontal lamination (Mh, Sh), or with massive structure (Mm, Sm), or with asymmetrical ripple lamination (Sr); they are characterized by low bioturbation indexes (BI = 0–2) related to *Teichichnus* and *Thalassinoides*, by syneresis cracks (Ms), siderite nodules, and organic debris, and by an absence of marine calcareous microfossils (Fig. 5D; Table 3). FA2 (fluvial-dominated prodelta) presents a gradual transition to FA4 (fluvial-dominated distal delta front).

4.3.2.1. Interpretation: fluvial-dominated prodelta. The record of Mm and marine calcareous microfossils and the low bioturbation (BI = 0–1; *Planolites*) are interpreted as sediments deposited by low-energy suspension fallout of fine-grained sediments during fair-weather conditions in offshore environments with low oxygenation or benthic food availability. However, the occasional occurrence of Sng and the recovery of palynomorphs could be related to seasonal muddy hyperpycnal flows originating at the river mouth during floods/torrential rains and moving a volume of clastic sediments farther prodelta/offshore (Lamb and Mohrig, 2009; Zavala et al., 2016; Zavala, 2020; Chalabe et al., 2022). The presence of *Phycosiphon* (BI = 4–5) thus reveals an eventual increase in benthic food and oxygen linked to the variable area influenced by hyperpycnal flows. The transition toward the top to Mm, Sm, Mh, Sh, and Sr, with *Teichichnus* and *Thalassinoides*, is interpreted as deposited

Table 2
Relationship between lithofacies and facies associations (FA).

Facies Code	FA1	FA2	FA3	FA4	FA5	FA6	FA7	FA8	FA9	FA10	FA11	FA12
Gmm						10%					~25%	
Gcm						5%						
Gng						15%						
Sig						10%		~5%				
Sng		~5%						~20%				
Sm		~5%	~10%	~30%	~25%	25%	~45%	~35%			~40%	25%
Sh		~10%	~5%	~10%	~5%	10%	~10%	~10%			~10%	
Sa											~5%	
Sp				~20%	~10%	10%	~20%				~10%	15%
St						5%	~5%	~7,5%				
Sr		~5%		~10%	~5%	5%	~10%	~15%		~5%	~10%	
Sw			~15%		~10%							
Sc			~5%			5%				~5%		
Shcs			~5%		~5%		~2,5%					
Ss			~5%		~5%		~2,5%					
Htf									~40%			
Htw									~30%			
Htl									~20%	~10%		
Slc, Sf								~2,5%				
Mm		~35%	~45%	~30%	~35%		~5%		~10%	~40%		
Mh		~35%	~10%					~5%		~10%		15%
Ms		~5%								~5%		
Cm												40%
Col										~20%		5%
Com										~5%		
Gbm	~25%											
Sbm	~65%											
Mbm	~10%											

from dilute river-derived turbidity currents (hyperpycnal flows) with organic debris transported in suspension. The low diversity of trace fossils, high content in palynomorphs, syneresis cracks, and siderite nodules reveal salinity fluctuations associated with freshwater fluvial domination (MacEachern et al., 2005).

4.3.3. Facies association 3 (FA3)

Description: FA3 is recognized by thick beds (31–100 cm) of structureless mudrocks (Mm), as well as intercalations of mudrocks and fine-grained sandstones occasionally with symmetric ripple lamination (Sw). Horizontally laminated mudrocks (Mh) interbedded with medium to thick beds of structureless sandy mudrocks (Sm), and fine-grained sandstones with horizontal lamination (Sh) also are observed. Moreover, there are scarce fine-grained sandstones with micro-hummocky cross-stratification (Shcs), micro-swaley cross-stratification (Ss), and soft-sediment deformation structure (Sc). This successions reach up to ~15 m tick. The bioturbation index ranges goes from low to moderate (BI = 0–4) with *Ophiomorpha*, *Planolites*, *Siphonichnus*, *Teichichnus*, and *Thalassinoides*. Also recognized in this facies is a high abundance of dinoflagellates and foraminifera, and moderate abundance of calcareous nannofossils. Fragments of bivalves, gastropods, and shell hash also occur (Fig. 5E and F; Table 3). FA3 (mixed prodelta) shows a transitional gradation to FA5 (mixed distal delta front).

4.3.3.1. Interpretation: mixed prodelta. The dominance of Mm, and the subordination of Sw, with variable bioturbation indexes (BI = 0–4; *Ophiomorpha*, *Planolites*, *Siphonichnus*, *Teichichnus*, and *Thalassisnoides*), along with the high abundance of marine microfossils, the fragments of bivalves and gastropods, and the presence of shell hash all suggest marine conditions at the lower limit of fair-weather wave base level in a prodelta–distal delta front/offshore environment domination (MacEachern et al., 2005).

Mh, interbedded with Sm, and Sh may represent unconfined lobes in the distal domain of turbidity current deposits (hyperpycnites; Zavala et al., 2011).

Occasionally, the record of Shcs/Ss, and of Sc not associated with bioturbation, could signal storm episodes below a fair-weather wave base affecting previous conditions (Arnott and Southard, 1990). The continuous progradation to shallower facies impedes the interpretation as a wave-dominated environment (shoreface to offshore), pointing instead to a mixed fluvial-wave prodelta system (Dalrymple et al., 1990, 1992; Shchepetkina et al., 2019).

4.3.4. Facies association 4 (FA4)

Description: FA4 is composed of medium to thick beds (11–100 cm) of mudrocks (Mm), muddy sandstones, and coarsening-upward trend to sandstones with massive structure (Sm), planar cross-bedding (Sp), asymmetric ripple lamination (Sr), horizontal lamination (Sh), and low to moderate bioturbation indexes (BI = 0–3) linked to *Ophiomorpha*, *Taenidium*, and *Thalassinoides*, with a sparse record of calcareous

microfossils, occasionally morichal palms, and organic debris (Fig. 5G and H; Table 3). This successions reach thicknesses of up to ~6 m. FA4 (fluvial-dominated distal delta front) displays a gradual shift to FA6 (fluvial-dominated mouth bar).

4.3.4.1. Interpretation: fluvial-dominated distal delta front. Coarsening-upward trends above represent a progradation and a transitional evolution of different tractive sedimentary structures within the sandstones, indicating fluctuating velocity in sustained turbulent flows (Gamero Diaz et al., 2011). All these features, together with the low to moderate bioturbation indexes (BI = 0–3; *Ophiomorpha*, *Taenidium*, and *Thalassinoides*) and the scarcity of marine calcareous microfossils (FA4), suggest more proximal environments within the deltaic system than the two previous FAs (MacEachern et al., 2005; Gingras et al., 2011). Absence of dwelling structures of suspension-feeding organisms, low ichnodiversity, variable concentrations of organic debris, and a prograding trend from sustained turbulent flows may reflect fluvial currents in a fluvial-dominated distal delta-front, associated with the collapse of mouth-bar deposits (MacEachern et al., 2005; Bhattacharya and MacEachern, 2009).

4.3.5. Facies association 5 (FA5)

Description: FA5 consists of thick beds (31–100 cm) of muddy sandstones and a coarsening-upward trend to fine-to medium-grained sandstones with massive structure (Mm, Sm) and symmetric ripple lamination (Sw), that reach thicknesses of up to ~4.5 m. These facies show low to high bioturbation indexes (BI = 0–5), with *Diplocraterion*, *Ophiomorpha*, *Planolites*, *Teichichnus*, and *Thalassinoides*, and some calcareous microfossils (Fig. 5I and J; Table 3). In addition, there are medium to thick beds of fine-to medium-grained sandstones with planar cross-bedding (Sp), asymmetric ripple lamination (Sr) or horizontal lamination (Sh), and a decrease in bioturbation indexes (BI = 0–2; *Ophiomorpha*). To a lesser extent, micro-hummocky cross-stratification (Shcs) and micro-swaley cross-stratification (Ss) can also be observed. FA5 (mixed distal delta front) exhibits transitional variation to FA7 (fluvial-, wave- and storm-influenced mouth bar).

4.3.5.1. Interpretation: mixed distal delta front. The coarsening-upward trend from Mm to Sm in addition to Sw, the low to high bioturbation indexes (BI = 0–5; *Diplocraterion*, *Ophiomorpha*, *Planolites*, *Teichichnus*, *Thalassinoides*), and the presence of dinoflagellates, foraminifera, and calcareous nannofossils (FA5) may reflect an environment controlled by fair-weather waves, characteristic of the distal delta front (MacEachern et al., 2005; Bhattacharya, 2006; Moyano-Paz et al., 2020). These lithofacies are interbedded with Sp and Sh that locally show Sr, and they display a decrease in the diversity and abundance of trace fossils (BI = 0–2; *Ophiomorpha*). These features reveal a continuous fluvial influence and therefore evidence a mixed system (e.g., Bhattacharya, and Giosan, 2003; Bayet-Goll and Neto de Carvalho, 2020). Beds with Shcs, Ss, and non-bioturbation suggest storm episodes (Arnott and Southard, 1990; Pemberton et al., 1992).

4.3.6. Facies association 6 (FA6)

Description: FA6 consists of thick beds (31–100 cm) resulting in successions up to ~3 m of medium-to coarse-grained sandstones with massive structure (Sm), and conglomeratic sandstones with horizontal lamination (Sh). Also seen are inverse grading and bigradational trends from thick beds of coarse-grained sandstones to conglomeratic coarse-grained sandstones and granule- and pebble-size conglomerates that are matrix-supported (Gmm-Gng; Gcm-Sig; Fig. 6A). The clasts are angular to very angular with low sphericity, and the matrix is medium-to coarse-grained sand without organic debris. Thick beds of fine-to

Table 3
Summary of the main features of the facies associations recognized.

Facies Association	Lithology	Simple facies codes	Ichnology	Micropaleontology	Interpretation
FA1	Bioclastic sediments (bioclastic conglomerates, bioclastic sandstones, bioclastic mudrocks).	Sbm, Gbm, Mbm.	*Ophiomorpha* (BI = 0-3).	Bivalves, gastropods (*Aclis* spp., *Turritella* spp.), scaphopod fragments, and indeterminate shells.	Transgressive lag
FA2	Mudrocks, and intercalation of mudrocks, sandy mudrocks and fine-grained sandstones.	Mm, Mh, Sh, Sr, Sm, Sng, Ms, and siderite nodules.	BI = 0-1; *Planolites* and exclusive presence of *Phycosiphon* where the bioturbation index increases (BI = 4-5). BI = 0-2; *Teichichnus*, and *Thalassinoides*.	Some foraminifera and calcareous nannofossils, as well as, palynomorphs.	Fluvial-dominated prodelta
FA3	Mudrocks, sandy mudrocks, intercalation of mudrocks, and fine-grained sandstones.	Mm, Sw. Mh, Sm, Sh. Shcs, Ss, Sc.	BI = 0-4; *Ophiomorpha*, *Planolites*, *Siponichnus*, *Teichichnus*, *Thalassisnoides*.	Abundant dinoflagellates (*Lingulodinium* spp.), foraminifera, and moderate amounts of calcareous nannofossils, besides bivalves and gastropod fragments as well as undifferentiated shell hash.	Mixed prodelta (fluvial, wave, and storm influence)
FA4	Muddy sandstones and fine- to medium-grained sandstones.	Mm, Sm, Sp, Sr, Sh.	BI = 0-3; *Ophiomorpha*, *Taenidium*, and *Thalassinoides*.	Calcareous microfossils (foraminifera and calcareous nannofossils) in low proportions. Occasionally morichal palms.	Fluvial-dominated distal delta front
FA5	Coarsening upward trends from muddy sandstones to fine- medium-grained sandstones.	Mm, Sm, Sw. Sp, Sr, Sh. Shcs, Ss.	BI = 0-5; *Diplocraterion*, *Ophiomorpha*, *Planolites*, *Teichichnus*, *Thalassinoides*. BI =0-2; *Ophiomorpha*.	Some calcareous microfossils (foraminifera and calcareous nannofossils).	Mixed distal delta-front (fluvial, wave, and storm influence)

FA6	Fine- to coarse-grained sandstones and the occurrence of organic debris highlighting lamination. Coarse-grained sandstones, conglomeratic coarse-grained sandstones and granule- and pebble-size conglomerates without the presence of organic debris, with floating clasts and granules. On some occasions, the conglomerates present, towards the top, variations to medium- fine-grained sandstones.	Sm, Gmm-Gng, Gcm-Sig, Sp, Sh, St, Sr, Sc.	Trace fossils are usually absent (BI = 0).	Abundant pollen and spores.	Proximal delta front (fluvial-dominated mouth-bar)
FA7	Fine- medium- to coarse-grained sandstones with occasional organic debris.	Sm, Sp, St, Sh, Sr. Sm, Shcs, Ss.	BI = 0-3; ichnological association or the exclusive presence of *Dactyloidites*, *Macaronichnus*, *Ophiomorpha*, *Skolithos* and / or *Thalassinoides*. Or BI = 0-5; ,?Asterosoma, *Conichnus*, *Cylindrichnus*, *Dactyloidites*, *Macaronichnus*, *Ophiomorpha*, *Skolithos*, *Thalassinoides*.	Pollen and spores are common, and some calcareous microfossils.	Proximal delta front (fluvial- wave- and storm-influenced mouth bar)
FA8	Granule-size conglomerates, conglomeratic medium-grained sandstones, and medium- to coarse-grained sandstones with high content of organic debris.	Sm, Sng, Sig, Sh, Sr, St, Slc, Sf, Mh and erosive bases.	BI = 0-2; exclusive presence of *Ophiomorpha* or *Taenidium*.	Abundant pollen and spores.	Lower delta plain (terminal distributary channel)
FA9	Fine- medium- to coarse- grained sandstones. Some mudrocks and fine-grained sandstones interbedding.	Htf, Htw, Htl, Mm, mud-drapes.	There is no a trace fossil (BI = 0) record.	Continental palynomorphs such as pollen, spores, lowland forest, and fungi remnants.	Lower delta plain (Tidal-influenced distributary channel)
FA10	Mudrocks, muddy sandstones and intercalation of mudrocks and fine-grained sandstones, and coal seams. Rhythm of millimetric sheets of mudrocks and fine-grained sandstones with some micro soft-sediment deformation structure.	Mm, Col, Mh, Htl, Sr, Ms, siderite nodules, Com, and Sc.	BI = 0-2; *Teichichnus*, rhizoliths.	Abundant pollen and spores, fungi remnants and mangrove pollen (*Lanagiopollis crassa*), and occasional bivalves and gastropod fragments.	Lower delta plain (Water-logged interdistributary areas)
FA11	Granule-size conglomerates, conglomeratic medium-grained sandstones, and medium- to coarse-grained sandstones.	Sm, Gmm, Sp, Sh, Sr, Sa.	BI = 0.	–	Upper delta plain (Distributary channel)
FA12	Fine- to coarse-grained sandstones, some thin beds of mudrocks, coal seams and claystones.	Cm, Sm, Sp, Mh, Col.	BI = 0-3; rhizoliths.	Pollen and spores. Mangrove palynomorphs are scarce.	Upper delta plain (Crevasse splay and Floodplain)

medium-grained sandstones with planar cross-bedding (Sp), trough cross-bedding (St), and asymmetrical ripple lamination (Sr) are also observed (Table 3). The occurrence of organic debris highlighting the lamination is also common (Fig. 6B). Abundant pollen and spores were found in this facies association. On some occasions, the conglomerates present, towards the top, variations to medium- and fine-grained sandstones with soft-sediment deformation structure (Sc; Fig. 6C). Trace fossils are absent (BI = 0) (Table 3). FA6 (fluvial-dominated mouth bar) present transition contact to FA8 (terminal distributary channel).

4.3.6.1. Interpretation: fluvio-dominated mouth bar. The coarse-grained sandstones with massive structure (Sm), conglomeratic sandstones with Sh, and organic debris highlighting the lamination and abundant pollen and spores (FA6) are interpreted as a record of high-velocity currents, probably associated with bedload under hyperpycnal flow conditions during times of torrential rains. Sr, St, and Sp, could be associated with traction and suspended load during flow slowdowns in a low-flow regime (Mulder et al., 2003; Zavala et al., 2011; Slater et al., 2017).

Towards the top of the hyperpycnal deposits, thick beds of Sm, Gmm, Gng show a bigradational trend, with poorly sorted and angular clasts, sometimes overlain by Sc (FA6) that would be related to gravity flows (Shanmugam, 2009; Talling et al., 2012; Zavala, 2020). Deposits whose internal cohesion is the main grain support mechanism can transport a wide range of textural elements (up to giant blocks) floating in a matrix; they are generally associated with cohesive debris flows (Zavala, 2020). The high concentration of coarse and very coarse sand in the matrix of the studied deposits points to an intermediate stage between cohesive debris flow and hyperconcentrated flows (Zavala, 2020). The soft-sediment deformation structures observed could be related to water penetrating the plastic flow layer and becoming trapped in cavities beneath the bed, then escaping by bursting open the top of the cavity (Zavala, 2020; Shanmugam, 2021). They furthermore indicate rapid deposition and dewatering by loading, typical for mouth-bars in a delta front deposition (Bann et al., 2008; van Yperen et al., 2019; Cole et al., 2021). The angular to very angular clasts, lacking organic debris, are related to high-gradient settings with a source area very close to the coastline (Olariu and Bhattacharya, 2006; Zavala, 2020). Transition to FA8 can occur when the flow of water decreases and the river discharge is distributed in several smaller channels, forming a multi-channel delta.

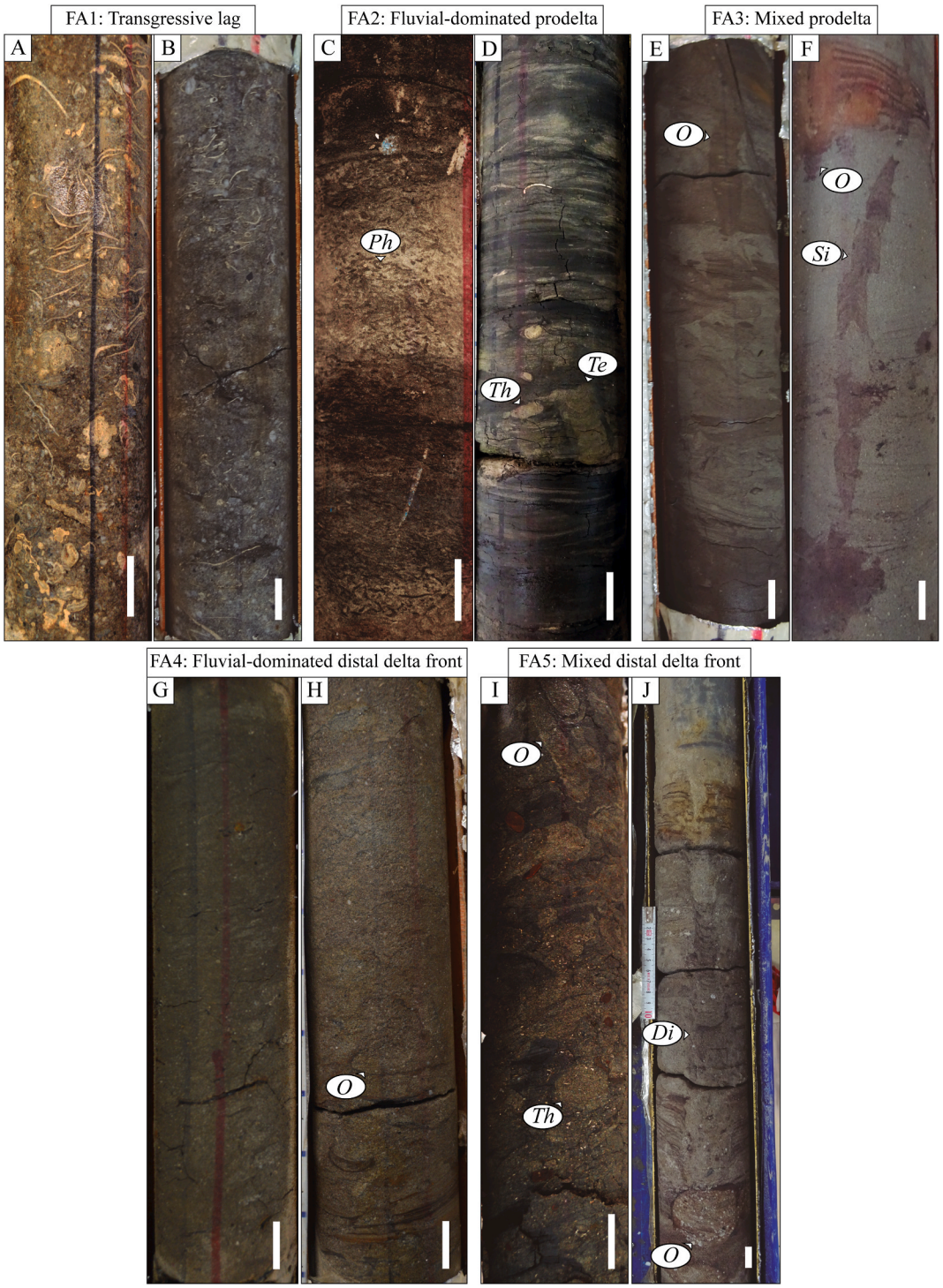

Fig. 5. Facies associatios FA1 to FA5. FA1: A. Structureless bioclastic sandstone. **B.** Structureless bioclastic conglomerate. **FA2: C.** Structureless mudrock and sandy mudrock with *Phycosiphon* (*Ph*). **D.** Laminated sandy mudrock interbedded with fine-grained sandstone with *Teichichnus* (*Te*) and *Thalassinoides* (*Th*), and bivalves. **FA3: E.** Laminated mudrock bioturbated by *Ophiomorpha* (*O*). **F.** Laminated **s**andy mudrock and fine-grained sandstone with *Ophiomorpha* (*O*) and *Siphonichnus* (*Si*). **FA4: G-H.** Bioturbated muddy sandstone with *Ophiomorpha* (*O*). **FA5: I.** Massive muddy sandstone highly bioturbated by *Ophiomorpha* (*O*) and *Thalassinoides* (*Th*). **J.** Laminated fine-grained sandstone with *Diplocraterion* (*Di*) and *Ophiomorpha* (*O*). Scale bar 2 cm.

In this context, the sedimentary succession can change from typical mouth-bar deposits, such as gravels and coarse sands, to finer and more laminated deposits associated with terminal distributary channels. Although the observed features are consistent with this interpretation, it is important to note that further analyses, such as additional core data or outcrop data, would be necessary to confirm and refine these interpretations.

4.3.7. Facies association 7 (FA7)

Description: FA7 encompasses thick beds (31–100 cm) resulting in succesions up to ~4.5 m of coarse-to fine-grained sandstones with massive structure (Sm), planar cross-bedding (Sp), trough cross-bedding (St), or horizontal lamination structures (Sh); with scarce organic debris; and/or with medium to thick beds to the top of sandstones with ripple lamination (Sr). Some sheets of mudrocks demarcate lamination. These

structures, but mainly massive sandstones, show low to high bioturbation indexes (BI = 0–5) and an ichnoassemblage consisting of ? *Asterosoma*, *Conichnus*, *Cylindrichnus*, *Dactyloidites*, *Macaronichnus*, *Ophiomorpha*, *Skolithos, Thalassinoides*, and some calcareous microfossils (Fig. 6D; Table 3). These succesions of ~4.5 m are interbedded with medium to thick beds of ~1–2 m thickness (planar contact) of coarse-to fine-grained sandstones that are structureless (Sm) or with planar cross-bedding (Sp) or trough cross-bedding (St); they contain organic debris and are bioturbated either by a trace fossil assemblage or by the exclusive presence of *Dactyloidites*, *Macaronichnus*, *Ophiomorpha*, *Skolithos* and/or *Thalassinoides* (BI = 0–3) (Fig. 6E). In the latter case, pollen and spores are common (Table 3).

Though less recurrent, also evident are medium beds of fine-to medium-grained sandstones with possible micro-swaley structure (Ss) and less abundant micro-hummocky cross-stratification (Shcs) where trace fossils are absent (BI = 0) (Fig. 6F; Table 3).

4.3.7.1. Interpretation: fluvial-, wave- and storm-influenced mouth bar. Sm, Sp, and Sh could indicate high-energy environments with sheet flows and migration of two-dimensional dunes (MacEachern et al., 2005; Coates and MacEachern, 2007). Presence of a diverse ichnoassemblage (?*Asterosoma*, *Conichnus*, *Cylindrichnus*, *Dactyloidites*, *Macaronichnus*, *Ophiomorpha*, *Skolithos,* and *Thalassinoides*; BI = 0–5) is evidence of high-energy marine conditions and most likely well-oxygenated waters. Thus, sheet flows and two-dimensional dunes, along with St, and Sr at the top, could indicate sandwaves (e.g., Davidson-Arnott and Van Heyningen, 2003) with possible wave reworking of temporary mouth-bar constructions probably during dry times (Bhattacharya, 2006; Olariu and Bhattacharya, 2006; Slater et al., 2017). However, these structures need to be detailed in the outcrop.

The interbedding of organic debris with beds of sandstones with Sm, Sp, St could be associated with traction load during flow slowdowns in a low-flow regime during wet times (Mulder et al., 2003; Zavala et al., 2011; Slater et al., 2017). Exclusive presence of *Dactyloidites*, *Macaronichnus*, *Ophiomorpha*, *Skolithos* and/or *Thalassinoides* (BI = 0–3) is evidence of decreased in abundance and diversity associated with increased sedimentation rates and possibly with changes in salinity.

Less abundant micro-Shcs, Ss, Sm, yet without bioturbation, are also related to unidirectional and oscillatory currents linked to storm and wave events (Arnott and Southard, 1990). The sedimentary environment energy, however, appears to have been much higher than that of the aforementioned conditions, and the development of bioturbation was inhibited. These aspects indicate high-energy deposition in a proximal mouth-bar setting with fluvial, wave, and storm influence (van Yperen et al., 2019).

4.3.8. Facies association 8 (FA8)

Description: FA8 is formed by thick beds (31–100 cm) of conglomeratic sandstones, and of sandstones with massive structure (Sm), normal grading (Sng), and inverse grading (Sig), with erosive bases resulting in sand- and conglomeratic sand bodies up to ~2.4 m. Moreover, there are thick beds of sandstones with horizontal lamination (Sh), ripple lamination (Sr), and trough cross-bedding (St). Some sandstones have load casts and flame structures (Slc/Sf), occasionally having a high content of organic debris; horizontal laminated mudrocks (Mh), and the exclusive presence of *Ophiomorpha* or *Taenidium* (BI = 0–2) are observed (Fig. 7A and B)Table 3. Generally, FA8 (terminal distributary channel) occurs after the recording of FA6 (fluvial-dominated mouth bar) or FA7 (fluvial-, wave- and storm-influenced mouth bar).

4.3.8.1. Interpretation: terminal distributary channel. A high content of organic debris, coarse-grained deposits with erosive bases (Sng, Sig), and bigradational trend, along with the exclusive presence of *Ophiomorpha* or *Taenidium* (BI = 0–2) (FA8), could attest to the influence of multiple subaqueous distributary channels providing hypopycnic conditions during normal fluvial discharge or hyperpychnic during

Fig. 6. Facies associations FA6 and FA7. FA6: A. Conglomeratic sandstone to conglomerate with coarsening-upward structure. **B.** Fine-to medium-grained sandstone with horizontal lamination highlighted by organic debris. **C.** Soft-sediment deformation structure in sandstone. **FA7: D.** Laminated fine-to medium-grained sandstone with some very thin beds of mudrocks bioturbated by *Conichnus* (*Co*) and *Ophiomorpha* (*O*). **E.** Interbedding of medium-grained sandstones and bioturbated mudrocks with *Skolithos* (*Sk*). **F.** Micro-hummocky and micro-swaley cross-stratification (dashed white lines) in sandstone. Scale bar 2 cm.

extraordinary river discharges (Bhattacharya and MacEachern, 2009; Buatois et al., 2011; Zavala et al., 2011; Zavala and Pan, 2018). This denotes more significant continental influence in the proximal delta front or lower delta plain. Such a situation would increase the input of freshwater into the environment in relation to the former FAs, and therefore substantially reduce salinity. Along with the increase in turbidity and sedimentation rate, this would prevent the development of macrobenthic communities, as described for the facies types of fluvial-dominated systems (Gingras et al., 1998; MacEachern et al., 2005). The interpretations associated with terminal distributary channels are based on the complete succession from the facies associations from mouth bars (FA6 and FA7). Because our interpretations about terminal distributary channel are limited to a single well-core, they should be confirmed with other well-cores or outcrops.

4.3.9. *Facies association 9 (FA9)*

Description: FA9 comprises thick beds (31–100 cm) of heterolithic beddings composed of medium-to fine-grained sandstones and

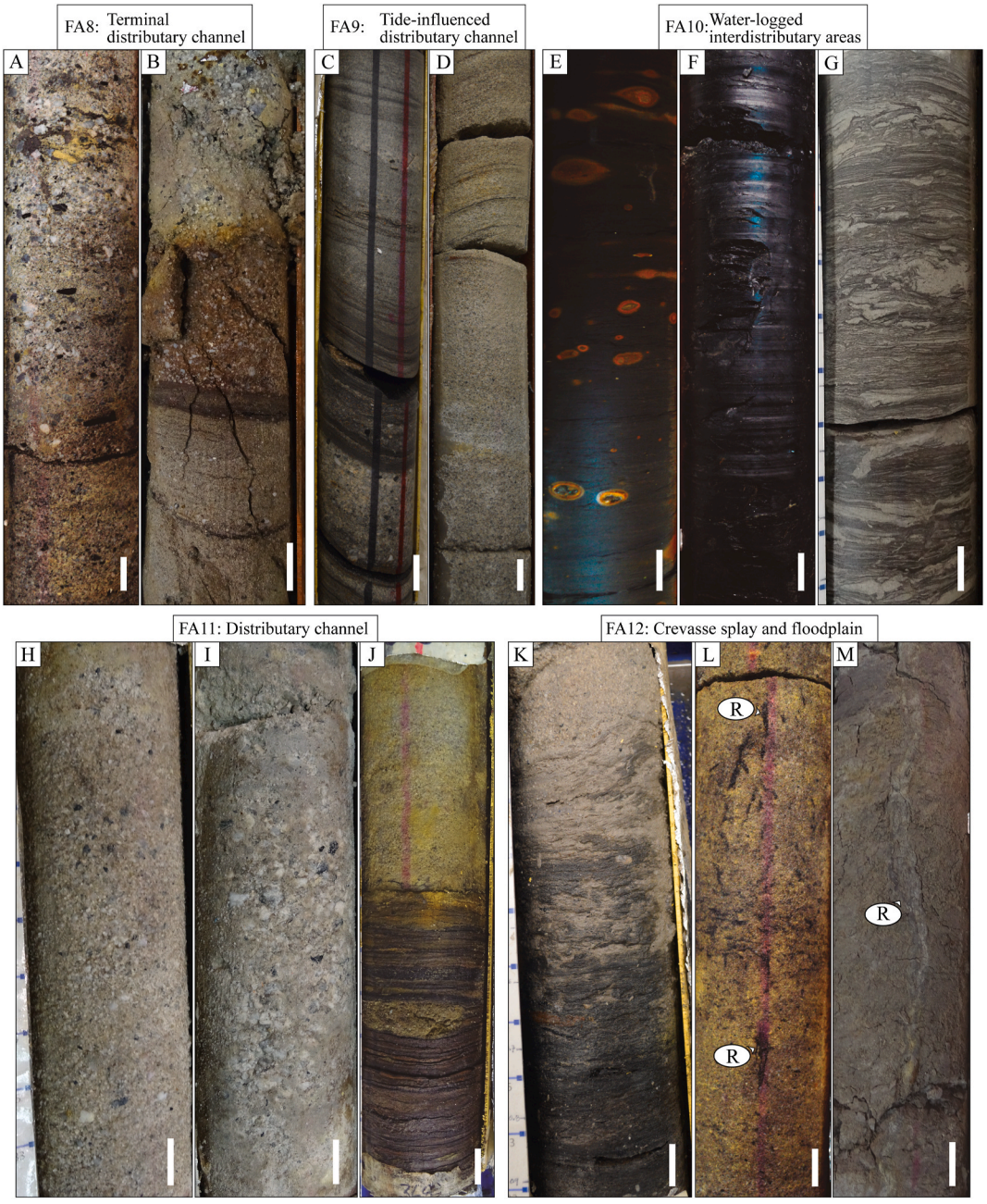

Fig. 7. Facies associations FA8 to FA12. FA8: A. Massive granule-size polymictic conglomerate (Gmm). **B.** Medium-grained sandstone with horizontal lamination (Sh) and sharp contact with coarse-grained sandstone to conglomeratic sandstone. **FA9: C.** Alternations of millimetric laminae of mudrocks and millimeter to centimeter intervals of sandstones and conglomeratic sandstones poorly selected with net base, sometimes erosive, and planar cross-bedding. **D.** Medium-grained sandstone with a massive structure (Sm) that varies transitionally to medium-grained sandstone with planar cross-bedding (Sp) highlighted by millimetric laminae of mudrocks. **FA10: E.** Horizontal laminated carbonaceous mudrock with ferruginous nodules (Mh). **F.** Laminated coal (Col). **G.** Alternation of millimetric laminae of mudrocks and fine-grained sandstones. **FA11: H.** Coarse-grained sandstone to conglomeratic sandstone with planar cross-bedding (Sp). **I.** Massive granule-size conglomerate (Gmm). **J.** Mudrock with lenticular bedding (Htf) overlain by medium-grained massive sandstone (Sm). **FA12: K.** Carbonaceous mudrock that varies transitionally to massive muddy to medium-grained sandstone (Sm). **L.** Massive sandstone with rhizoliths (R). **M.** Massive claystone with rhizoliths (R). Scale bar 2 cm.

mudrocks with a prevalence of flaser (Htf) out of wavy bedding (Htw), and some beds where the mud-drapes are very well registered. Reactivation surfaces are common. Structureless mudrock beds (Mm) are scarce, although their occurrence stands out in thin beds atop some FA6, which occasionally are part of lenticular beddings (Htl). Continental palynomorphs such as pollen and spores dominate, and lowland forests and fungi remnants are identified. Trace fossils are absent (BI = 0) (Fig. 7C and D; Table 3). On some occasions, FA6 (fluvial-dominated mouth bar) is intercalated with FA9. FA9 is restricted to interval I of the study section (Fig. 4).

4.3.9.1. Interpretation: tide-influenced distributary channel. The presence of Htf, Htw, and mud-drapes, together with the reactivation surfaces in sandstones, suggests cyclic sedimentation, probably associated with a bidirectional flow (Dalrymple et al., 1990, 1992; Dashtgard et al., 2009). The intercalation with FA6 indicates that tidal currents filled abandoned distributary channels (Martinius and Gowland, 2011). The scarcity of mudrocks in some intervals allows us to infer a generalized absence of slack water as well as the development of high-energy conditions (Dalrymple et al., 1990; Desjardins et al., 2012). Nonetheless, mudrock beds atop some FA6 with Htl support variations in fluvial discharge, even possible dropouts from the main channel (Gugliotta et al., 2016).

4.3.10. Facies association 10 (FA10)

Description: FA10 is made up of thick beds (31–100 cm) resulting in succesions up to ~2.4 m of structureless mudrocks (Mm), laminated mudrocks (Mh), and lenticular beddings (Htl) with asymmetric ripple lamination (Sr). Moreover, syneresis cracks (Ms) and siderite nodules are common (Fig. 7E), showing low bioturbation indexes (BI = 0–2) associated with *Teichichnus* and rhizoliths. Locally, bivalves and gastropod fragments, along with abundant pollen and spores, fungal remnants, and mangrove pollen, are recorded (Table 3). Also common in FA10 are medium to thick beds (11–100 cm) of laminate coals seams (Col) and structureless coal (Cm), on some occasions with rhizoliths (BI = 0–2) (Fig. 7F; Table 3). Alternations of millimetric laminae of mudrocks and fine-grained sandstones are also recorded (Fig. 7G).

4.3.10.1. Interpretation: water-logged interdistributary areas. Altogether, the record of Mm, Mh, Ms, siderite nodules, low bioturbation indexes, and abundant fungal remnants clearly suggest low-energy accumulation zones in brackish-water conditions. The record of Htl and Sr and the alternation of millimetric mudrocks and sandstone with marine bivalve and gastropod fragments as well as *Teichichnus* suggest cyclic sedimentation, probably associated with a bidirectional flow in interdistributary bays (Rossi and Steel, 2016). The presence of coal seams and Mm with rhizoliths (BI = 0–2) attest to the development of peat bogs in swampy areas. Constantly waterlogged conditions would have enabled both the accumulation and preservation of organic matter subjected to reducing conditions (Retallack, 2001).

4.3.11. Facies association 11 (FA11)

Description FA11 comprises thick beds (31–100 cm) generating successions up to ~3 m thick composed of fining-upward trend from conglomerates, conglomeratic medium-grained sandstones, coarse-grained sandstones with massive structure (Sm; Gmm), to medium-grained sandstones with horizontal bedding (Sh), planar cross-bedding (Sp), asymmetric ripples (Sr), and low-angle cross-bedding (Sa), without bioturbation (Fig. 7H-I-J; Table 3). FA11 is restricted to interval III of the study section.

4.3.11.1. Interpretation: distributary channel. Thickly bedded Sp, Sh, Sa, and Sr, all without evidence of bioturbation are originate in high-energy currents that force the migration of bottom forms (dunes) associated with fill of channel successions, where Gmm, Sm, represent the base of channel (Einsele, 2000; Miall, 2014). The dunes may partially represent bars associated with fluvial channels that transported sediment as bottom load, and the fining-upward pattern may be related to lateral migration and sudden abandonment of the canals by avulsion (Einsele, 2000). There is no evidence of marine influence in the system.

4.3.12. Facies association 12 (FA12)

Description FA12 is represented by medium to thick beds (31–100 cm), which cumulatively may reach thicknesses of up to ~45 m, of fine- to coarse-grained sandstones with planar cross-bedding (Sp), as well as thin, horizontally laminated mudrock beds (Mh) and massive fine-grained sandstones (Sm) (Fig. 7K) that occasionally contain rhizoliths (BI = 0–3) (Fig. 7L); also found in FA are medium to thick beds of massive claystones (Cm) and laminated coals (Col) with rhizoliths (BI = 0–1) (Fig. 7M). Pollen and spores are recorded, and mangrove palynomorphs are scarce (Table 3). FA12 is restricted to interval III of the study section.

4.3.12.1. Interpretation: crevasse splay and foodplains. Sandstones, coals, and claystones with rhizoliths suggest deposition during alternating high- and low-energy conditions associated with crevasse splay deposits (e.g., dikes or overflows), and floodplains. Such environments are relatively distant from the channel and tend to accumulate sediments during and after floods when the river breaks its natural levees (Selley, 1985; Einsele, 2000; Esperante et al., 2021). Sandstone beds with rhizoliths mark the cessation of current discharge and establishment of permanent vegetation (Retallack, 2001; Bridge, 2006). From the presence of Cm with rhizoliths (BI = 0–1) and mottled textures (FA12) we can infer relatively low-energy conditions associated with vast floodplains and soil development, recording prolonged subaerial exposure (Makaske, 2001; Retallack, 2001; Miall, 2014).

5. Depositional systems and evolution

The established chrono-stratigraphic framework and detailed sedimentological, ichnological, and micropaleontological results allow us to interpret the temporal evolution of the sedimentary settings. Three different intervals are recognized in the cored section (Fig. 4). The lowest, interval I, comprises FA6, FA7, FA8, and FA9 (Fig. 8A). Facies associations from FA1 to FA10 are components of intervals II and III. Assemblages of FA11 and FA12 are identified in the upper part of the section, helping to distinguish interval II from interval III (Fig. 8B and C). We therefore propose the following succession: (i) a setting likely controlled by fluvial-dominated and tide- or wave-influenced mouth-bars in the middle-late Eocene? to early Oligocene (interval I); (ii) subsequent development of a fine-grained deltaic system initially mixed and influenced by river, waves, and storms during most of the Oligocene (interval II); and finally (iii) a general mixed fine-grained deltaic system, with aggradation of continental and marine systems, that stabilizes toward the end of the Oligocene/Early Miocene (interval III) (Fig. 8).

5.1. Interval I – middle-late Eocene? to early Oligocene: fluvial-dominated coarse-grained delta with wave- and tidal-influenced

Interval I corresponds roughly to ~691–614 m at the base of the studied section (Fig. 4). A succession of facies with an aggradational trend is marked by an alternation of facies from FA6 to FA9 (Fig. 8A). This succession features hyperpycnal-dominated mouth bars (FA6), followed by hyperconcentrated flows (FA6, FA8; Fig. 8A). FA7 reveals environmental variations, notably an increase in the influence of waves and sometimes conditions allowing macrobenthic activity (*Ophiomorpha*) (Fig. 8A). The record of tide-influenced distributary channels (FA9) at the top of some alternations suggests a filling of abandoned distributary channels through the action of tides (Fig. 8A) (e.g., Johnson and Dashtgard, 2014; Dalrymple et al., 2015).

A coarsening-upward succession of facies types FA6 to FA9 repeats

along this interval, without the periodic occurrence of FA7 (zoom interval I, Fig. 8A). The thickness of this zoom succession is ~3–5 m associated with amalgamated mouth bars settings.

During the middle-late Eocene? to early Oligocene, then, we see aggradational trend successions that indicate high-energy deposition indicative of distributary channels and mouth-bars settings, most likely within a coarse-grained delta (Olariu and Bhattacharya, 2006; Enge et al., 2010; van Yperen et al., 2019; Cole et al., 2021). Contributions

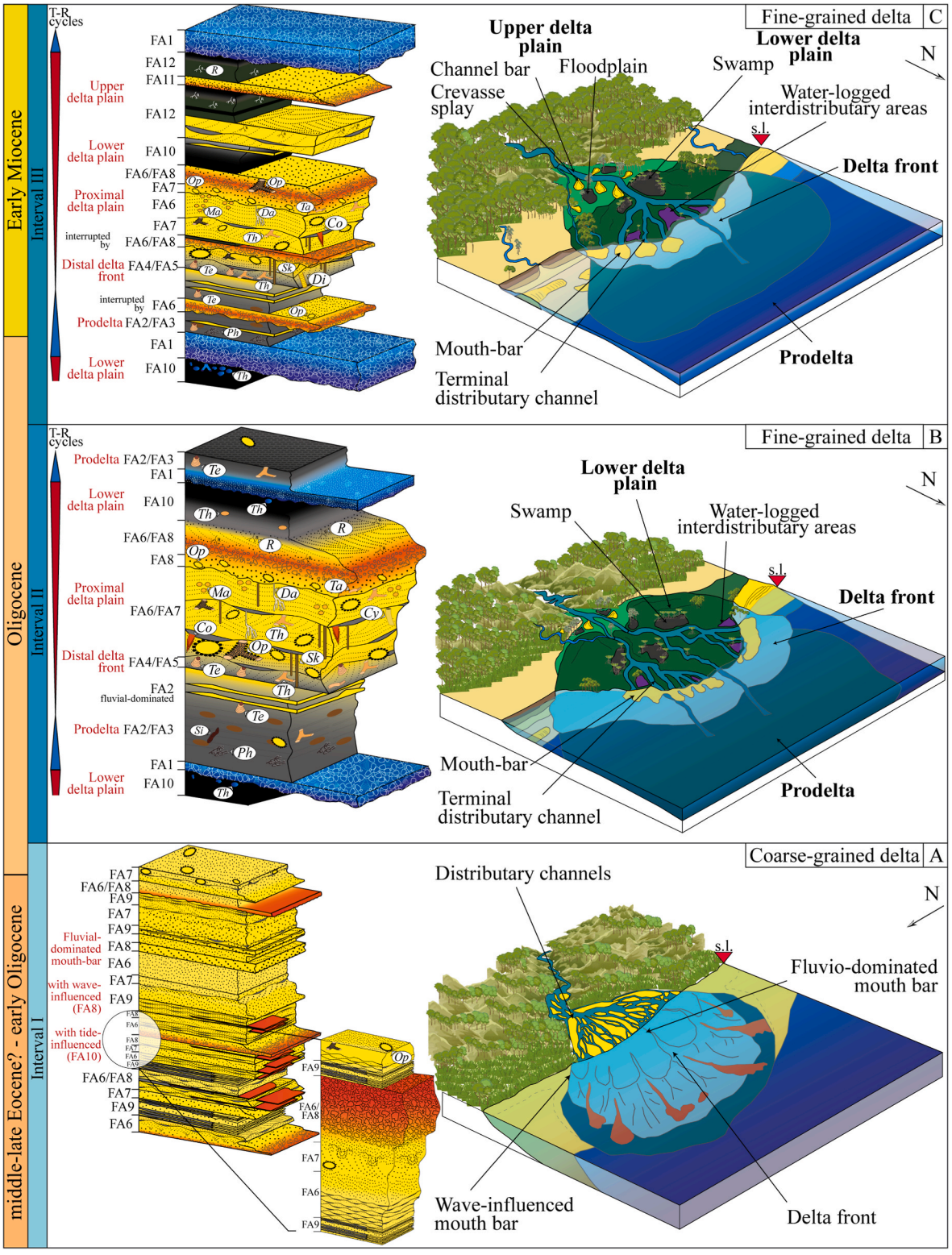

Fig. 8. Succession of facies types for intervals I to III, evolution of sedimentary settings, and a sketch of the interpreted evolution of the coastline from the middle-late Eocene? to the Early Miocene in the area represented by the studied core. s.l.: sea-level. **A.** Interval I: Succession of the mouth-bar to distributary channel units of river-dominated, tidal- and wave-influenced mouth-bar type delta. **B.** Interval II: Sequence of facies types of deltaic system for the succession of the interval II. **C.** Interval III: Sequence of facies types of deltaic system frequently interrupted by the progradation of continental systems.

from wet tropical lowland forests are inferred from continental palynomorphs such as pollen and spores. Rapid avulsions and lateral displacements of channels (probably high gradient) would have prevented the development of interdistributary bays and swamps (lower delta plain). This interaction of fan deposits and forests has been characterized in other stratigraphical sequences (e.g., Wilford et al., 2005).

Under the high-energy conditions generated by hyperpycnal and hyperconcentrated flows from short river systems, biogenic structures were either not produced or not preserved due to excessive background instability (BI = 0) (Gani et al., 2007; Gingras and MacEachern, 2012). Even a short period of wave or tidal influence may prevent the develop of trace fossils in a sedimentary environment, a re-working of mouth-bars by waves, absent the influence of gravity flows for a considerable time, could, however, generate conditions more favorable for the record of bioturbation at the end of the interval I (from ~645 m). In sum, trace fossils in this period likely were affected by both hydrodynamic conditions and changes in salinity. Increased sedimentation rates further impede the construction and maintenance of permanent domiciles by benthic organisms. The result is a reduced concentration of food resources per unit volume of sedimentary debris at the sea floor and rapid burial of sedimentary material beyond the reach of even deep-probing deposit feeders (MacEachern et al., 2005).

5.2. Interval II - Oligocene: mixed fine-grained deltaic environment (fluvial, wave, and storm influenced)

The transition zone to interval II (~614 m) is marked by a drastic reduction of hyperconcentrated flows and amalgamated successions of mouth-bars. The change is driven by a sudden marine transgression that overlies the previous facies. The first record of FA2 shows the onset of hyperpycnal prodelta development and the prograding fluvial system that restarted after transgressions (FA1 – transgressive cycles; Fig. 4). This zone is also characterized by a sudden increase in fungal remnants, suggesting that swamps and interdistributary bays occupied the proximal part of the sedimentary system. For this reason, the distributary channels and mouth-bars had greater stability (Fig. 8B).

Interval II, corresponding to ~614 m to ~297 m (Fig. 4), displays alternating progradational trends to form a succession facies type (Fig. 8B). This succession may show coarsening-upward fluvial dominance (FA2-FA4-FA6) up to 46 m thick or coarsening-upward of a mixed system (FA3-FA5-FA7) up to ~24–30 m thick. It always ends in terminal distributary channels (FA8) and water-logged interdistributary areas (FA10); we thus see the alternation of transgressive cycles (F1) and regressive cycles (T-R cycles Fig. 4; 8 B–C). Deposits with erosive bases, high organic debris, and coal beds (FA6 to FA8) can be linked to classical deltaic sequences (Ainsworth et al., 2017; Shchepetkina et al., 2019; Maselli et al., 2020). The FA8 and FA10 always restarted in the wake of transgressive lags with *Glossifungites* ichnofacies at the base (FA1), typical of firm substrates exhumed by erosion during a transgression phase that determines ravinement surfaces (T-R cycles; Fig. 4; Fig. 8B and C). Such features led us to interpret a generalized mixed deltaic environment for interval II, varying between fluvial-dominated phases and others more significantly influenced by waves and storms (in both scenerios from prodelta to lower delta plain–succession facies type) (e.g., Dashtgard and La Croix, 2015; Rossi and Steel, 2016; Rossi et al., 2017). The high abundance of morichal palm pollen suggests gallery flood forests close to the transitional system. Therefore, the beginning of these regular alternations with erosive bases associated with FA1 to FA10 marks interval II and its boundary with interval I; here the delta widens, reducing the gradient and developing a greater lower delta plain with more stable sub-environments than in interval I.

The evolution of fresh/brackish/marine salinity settings generated by this intensive interaction between the fluvial-deltaic system had a direct impact on the macrobenthic tracemaker communities (Gingras et al., 1999; MacEachern et al., 2005; Bhattacharya and MacEachern, 2009). The fluvial discharge likely ranged from hyperpycnal to homopycnal; such changes may be temporally variable, especially in tropical conditions (Warne et al., 2002; Buatois et al., 2012). Higher fluvial discharges are generally characterized by elevated sedimentation rates in proximal positions, resulting in lower bioturbation intensities as evidenced in the interpreted lower delta plain. Still, salinity exerts first-order control upon benthic fauna (Díez-Canseco et al., 2015). Other stress factors, e.g., hypopycnal conditions, commonly result in the development of buoyant mud plumes that extend from the delta front to the prodelta region. This clear influence of the deltaic plumes in the sequence of facies types is evident. It drives the decrease of abundance and diversity of the macrobenthic tracemaker communities when water turbidity increases and there is freshwater input in the system (e.g., Warne et al., 2002). In sum, this sequence of facies types develops from the prodelta to the proximal delta front with fluvial-dominated input and higher specific recovery of palynomorphs. Meanwhile, the infaunal diversity, abundance, feeding strategy, and overall behaviors increase drastically when there is a mixed influence (waves and rivers).

5.3. Interval III – late Oligocene to Early Miocene: mixed deltaic environment (fluvial, wave, and storm influenced) with aggradation of continental and marine systems

Interval III, corresponding to ~297–0 m (Fig. 4), bears similarities with interval II, e.g., the repetitive record from prodelta to lower delta plain settings of the facies successions (Fig. 8B and C). In the transition zone and during the first stages of interval III, rapid changes between regressive and transgressive cycles stand out, revealing some instability in the fluvial-deltaic system (Fig. 4; 8 B–C). However, a subsequent and more significant aggradational trend in the continental environment is apparent (FA11 and FA12). Interval III is further differentiated by its diverse frequency of facies associations and by sedimentological and ichnological differences from interval II. Thus, distributary channels (FA11) to crevasse splay and floodplains (FA12) occur above terminal distributary channels (FA8) to water-logged interdistributary areas (FA10), thus indicating the end of the succession facies types in this interval. Then, the more frequent FA6 and FA8, and the less frequent FA2-FA4 and FA3-FA5, lead us to infer a progradation of continental deposits (Fig. 8C). A distinctive feature of interval III is the continuous repetition of FA11 to FA12 associated with an aggradational continental sedimentation (upper delta plain) into the fluvio-deltaic system with vast floodplains and soil development, indicating prolonged subaerial exposure. An increase in mangrove pollen (*Zonocostites* and *Lanagiopollis crassa*) supports the establishment of a transitional environment in this interval. The record of continental facies is interpreted as evidence that the upper delta plain continues to increase, at least from ~221 m (e.g., Bhattacharya, 2006; Hansen and MacEachern, 2007; Ainsworth et al., 2017; Collins et al., 2019). Nevertheless, increased marine palynomorphs (dinoflagellates and foraminifera organic lining) and the development of a tracemaker community under mixed conditions (e.g., *Conichnus*, *Diplocraterion*, and *Ophiomorpha*) signal a higher significance of transgressive phases into interval III on the continental environment. We therefore interpret this as a general mixed deltaic system similar to interval II, yet with a higher influence of fluvial-dominated processes and recurrence of wave processes. Aggradation of continental and marine systems stabilizes.

When a mixed system is established, trace fossil diversity is maximum in apparent normal salinity conditions associated with spikes of abundant dinoflagellates. It gradually decreases by diluting salinity in brackish water environments (upper and lower delta plain). Bioturbation varies, however, from sporadical distribution in the subaqueous distributary channels (mouth bar) to a remarkable paucity associated with fully upper delta plain. In freshwater environments, an inland location could favor a secondary peak of diversity (Pemberton and Wightman, 1992; Buatois et al., 2005), although this is not evidenced in the studied record. The fluvial influence signal prevails in the studied system, and establishing control of other processes for long

periods is not possible. The influence of waves is noticeable in some intervals, but suddenly the ichnological and palynological signal reveals the entry of fluvial systems, modifying the previous conditions. Systems dominated by hyperpycnal prodeltas or mouth bars are created suddenly, probably in association with torrential rains.

6. Paleogeographic implications

Reconstructed hyperpycnal-dominated mouth-bar environments with hyperconcentrated flow input (coarse-grained deltas) in the context of the middle-late Eocene? and earliest Oligocene are correlated with the deposition of the San Jacinto Formation, interpreted as fan delta deposits by some authors (e.g., Guzmán, 2007 and references here contain; Mora-Bohórquez et al., 2020). Coarse-grained delta systems could be generated from nearby basement highs, as those were exhumed by that time. The sources of detritus would have been the orogen and magmatic arc at the south-southeastern of the well-core location (e.g., Cretaceous magmatic arc in the Central Cordillera) and the Magangué-Cicuco High (e.g., recycled sedimentary rocks exposed in the basement highs) to the east of the well-core location (Mora et al., 2017; Osorio-Granada et al., 2020). Moreover, the global eustatic curve for this period depicts a significant drop in sea level associated with the Eocene-Oligocene Transition (EOT) caused by the onset of the permanent ice sheet in Antarctica (Katz et al., 2008; Simmons et al., 2020; Hutchinson et al., 2021). This would point to a decrease in accommodation space, thereby suggesting some degree of correlation with amalgamated deposits (Interval I).

The sedimentary environments interpreted in this work reflect transitional variations in the final stages of gravity flow sedimentation during the middle-late Eocene?-early Oligocene, delimited by a transgression in the early Oligocene. In turn, palynology indicates the start of the lower delta plain supply system since that time. The prograding successions reveal the onset of fluvial/marine interaction, with more sediment accommodation space (fine-grained delta), which might be linked to the onset of subsidence processes reported by Mora-Bohórquez et al. (2020) in the Lower Magdalena Valley Basin. The identification of unconformities near the geological contact between the San Jacinto Formation and COF, as reported by Mora et al. (2017, 2018), is challenging due to limitations in biostratigraphic resolution. Additionally, the advance of continental systems with high sedimentation rates generates instability in marine systems (e.g., submarine slides, Mutti et al., 2003), and therefore unconformities would be registering only in more distal environments (e.g., Villegas et al. this volume). Moreover, these unconformities are difficult to document and estimate due to the lack of clear marine biostratigraphic markers in transitional environments.

We attribute the transition zone from coarse-grained delta upward to fine-grained delta in the early Oligocene to the continued increase in accommodation space in the basin during the Oligocene. This scenario, tied to the COF in the SW of the SJFB, might correspond to early phases of the proto-Cauca River delta development (at least from Amagá Formation), whose formation was driven by sedimentation from the Amagá fluvial system (the most important deltaic systems of the northern Andes during the Oligocene–Early Miocene). Detrital U/Pb geochronology data of Oligocene age from sandstones of Amagá (Lower Member) and Ciénaga de Oro Formations show similar signals in age populations (Lara et al., 2018; Manco-Garcés et al., 2020; Osorio-Granada et al., 2020, Fig. 9). In turn, contributions to the Lower Amagá member from Late Cretaceous igneous rocks from the Central and Western cordilleras, and Permo-Triassic metamorphic basement of the Central Cordillera have been recorded (e.g., Zapata et al., 2020). The interpretation of both cordilleras (Central and Western cordilleras) as source of sediments for the Amagá Formation in the Oligocene has also been based on interpretation of a north-trending paleocurrent direction for the river systems (Silva-Tamayo et al., 2008, 2020; Lara et al., 2018). The COF, during the Oligocene, has a source area from Lower Magdalena Valley Basin basement and/or Central Cordillera rocks and, to a lesser extent, from igneous rocks of the Western Cordillera (Mora et al., 2018; Manco-Garcés et al., 2020; Osorio-Granada et al., 2020). This interpretation is further supported by paleocurrents of rivers from south to north, and shorter systems from the east or southeast (Manco-Garcés et al., 2020) (Fig. 9).

The deltaic system interpreted in detail here for the late Oligocene to Early Miocene presents a greater aggradational trend. Therefore, the delta front could harbor a greater influence of waves, even showing delta aggradational tendencies (e.g., Moyano-Paz et al., 2022). Thus, because the accommodation space and sediment supply are unlikely to remain constant for any significant period, we would predict instead aggradation and stability of a possible fluvial-deltaic system such as the proto-Cauca River (at least from Amagá Formation), with a possible greater reworking of the waves in the delta front (Fig. 9). Previous authors invoke a regional unconformity at the top of the lower COF during the Early Middle Miocene (Mora et al., 2018). Our biostratigraphic data are inconclusive, and there is no physical evidence of this unconformity.

7. Conclusions

We used a multidisciplinary approach to study the influences on a mixed-energy deltaic setting on the SW Caribbean coast of Colombia during the middle-Eocene to Early Miocene. Our approach, using facies associations, trace fossils, and analysis of palynomorphs versus calcareous foraminifera/nannofossils from the well-core ANH-SSJ-Nueva Esperanza-1X, revealed a high variability of fluvial, wave, storm, and tidal processes, with long-term influence on this tropical deltaic environment. Twelve facies associations representing different deltaic subenvironments (from upper delta plain to prodelta), grouped in three stratigraphic intervals, show changes from the middle-late Eocene? to the Early Miocene. Interval I (middle-late Eocene? to early Oligocene) is represented by the amalgamation of hyperpycnal-dominated mouth bars with hyperconcentrated flow input capped by fine-grained, wave-influenced, and heterolythic deposits infilling distributary channels with land-derived palynomorphs. It is interpreted as the stacking of prograding units of fluvial-dominated, wave- and tide-influenced coarse-grained deltas, with humid tropical forest in the land and sources of sedimentation from nearby paleohighs. Our findings reveal a noteworthy impact of these high-energy conditions on the macrobenthic tracemaker community. Interval II (Oligocene) is represented by retrograding to prograding units of dominantly heterolythic deposits with a high content in morichal palm pollen alternating with thin transgressive lags. It is interpreted as flood-forested delta plain and hyperpycnal-dominated delta front to prodelta settings punctuated by transgressive wave pulses. Interval III (late Oligocene to Early Miocene) is represented by coal-bearing, thick, fine-grained packages containing mangrove pollen, and palaeosoils alternating with deposits showing the same facies associations as the underlying interval. It is interpreted as an aggradational, well-developed, flood-forested delta plain, commonly drowned during transgressions, thus allowing a tracemaker community to develop under mixed conditions. During the middle-late Eocene? to Early Miocene, the Colombian Caribbean presents the evolution from a steep, short, and presumably narrow margin (with coarse-grained deltas in coastal settings, interval I) to a more gentle and wide margin with a fine-grained delta (e.g., well-developed delta plain with swamps sporadically drowned, intervals II and III) reflecting both a long-term decrease in sediment supply, increase in accommodation ratio, and an increase of tropical flooded forests in the coastline associated with the evolution of perhaps the most important deltaic systems of the northern Andes during the Oligocene - Early Miocene (proto-Cauca river delta; at least from Amagá Formation). Sedimentological, ichnological, and micropaleontological analyses attempt to evaluate in detail the variations that may exist in the stratigraphic record within a tropical deltaic system, where it is complicated to determine dominant processes over long periods of time owing to the changing factors.

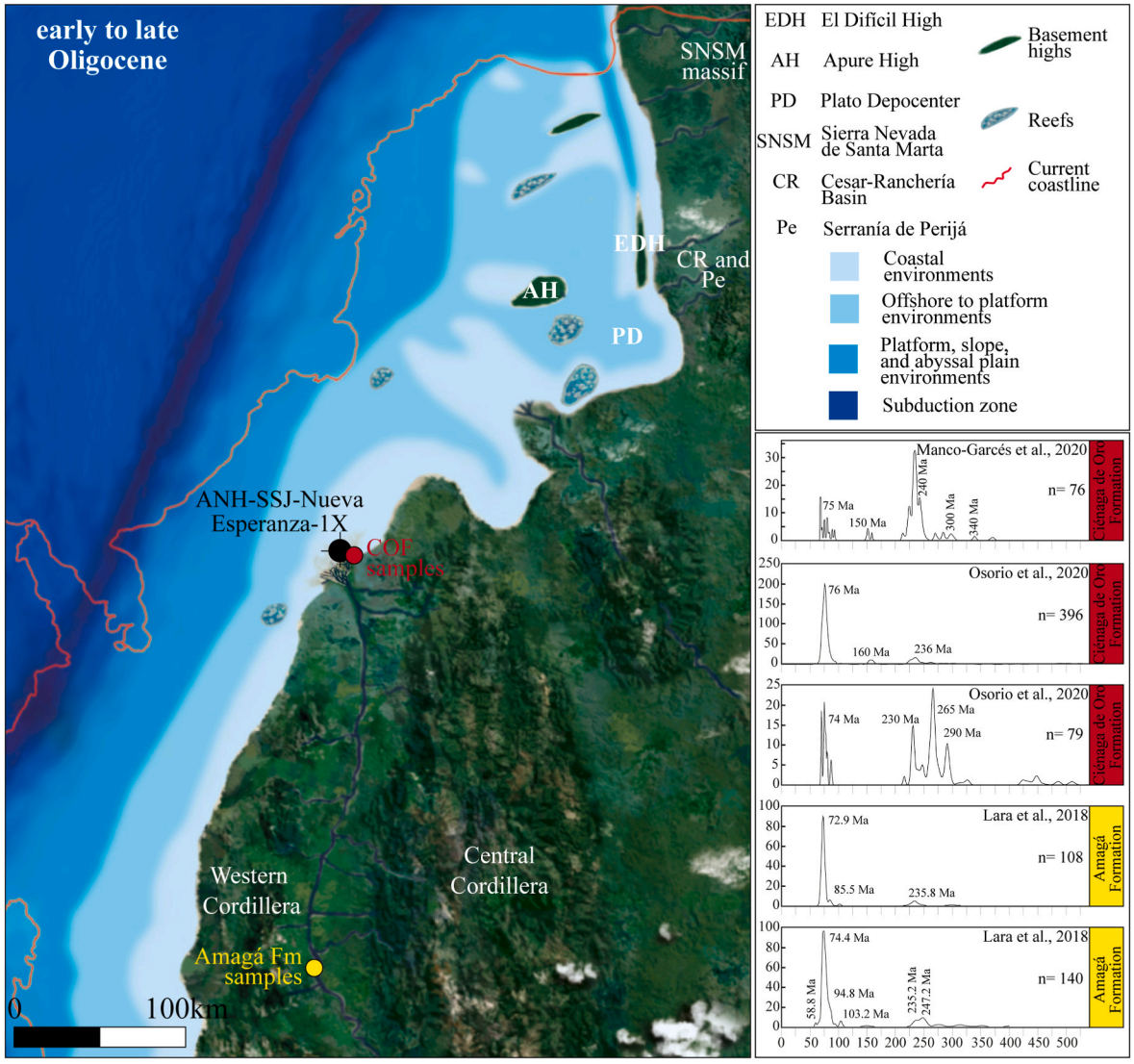

Fig. 9. Paleogeographic reconstruction of the proto-Cauca River delta in the SW SSJB during the early-late Oligocene. Detrital geochronology from Amagá Formation (Lara et al., 2018) and Ciénaga de Oro Formation (Manco-Garcés et al., 2020; Osorio-Granada et al., 2020). Modified from Mora et al. (2018).

Declaration of competing interest

The authors declare that they have no known competing financial interests or personal relationships that could have appeared to influence the work reported in this paper.

Data availability

Data will be made available on request.

Acknowledgements

The National Program for Doctoral Formation provided financial support to Celis and Giraldo-Villegas (Minciencias grants 885-2020, 906–2021, respectively). We want to thank the National Hydrocarbons Agency-ANH, and *Ministerio de Ciencia, Tecnología e Innovación - Minciencias* for allowing the study of well-core (Convenio 730/327–2016). The Vicerrectoría de Investigaciones y Posgrados and the Instituto de Investigaciones en Estratigrafía-IIES of Universidad de Caldas gave economic and logistic support. The research was conducted within the "Ichnology and Palaeoenvironment RG" (UGR). Financial support for Rodríguez-Tovar was provided by scientific Projects PID 2019-104625RB-100 (funded by MCIN/AEI/10.13039/501100011033), P18-RT- 4074 (funded by FEDER/Junta de Andalucía-Consejería de Economía y Conocimiento), B-RNM-072-UGR18 and A-RNM-368-UGR20 (funded by FEDER Andalucía). We want to thank to Dra. Beatriz Bádenas for constructive comments and suggestions on the earliest version of manuscript. Moreover, thanks to the editor Andrés Folguera and three anonymus reviewers for the comments and suggestions, which improved the manuscript. Funding for open access charge: Universidad de Granada / CBUA.

Appendix A. Supplementary data

Supplementary data to this article can be found online at https://doi.org/10.1016/j.jsames.2023.104368.

References

Agnini, C., Fornaciari, E., Raffi, I., Catanzariti, R., Pälike, H., Backman, J., Rio, D., 2014. Biozonation and biochronology of Paleogene calcareous nannofossils from low and middle latitudes. Newsl. Stratigr. 47, 131–181.

Ainsworth, R.B., Vakarelov, B.K., Nanson, R.A., 2011. Dynamic spatial and temporal prediction of changes in depositional processes on clastic shorelines: toward improved subsurface uncertainty reduction and management. APPG Bulletin 95, 267–297.

Ainsworth, R.B., Vakarelov, B.K., MacEachern, J.A., Rarity, F., Lane, T.I., Nanson, R.A., 2017. Anatomy of a shoreline regression: implications for the high–resolution stratigraphic architecture of deltas. J. Sediment. Res. 87, 425–459.
Arnott, R.W., Southard, J.B., 1990. Exploratory flow–duct experiments on combined–flow bed configurations, and some implications for interpreting storm event stratification. J. Sediment. Petrol. 60, 211–219.
Aubry, M.-P., 2014a. Cenozoic Coccolithophores: Discoasterales (CC-B). Micropaleontology Press. Atlas of Micropaleontology series, New York, p. 431.
Aubry, M.-P., 2014b. Cenozoic Coccolithophores: Discoasterales (CC-C). Micropaleontology Press. Atlas of Micropaleontology series, New York, p. 328.
Aubry, M.-P., 2015a. Cenozoic Coccolithophores: Discoasterales (CC-D). Micropaleontology Press. Atlas of Micropaleontology series, New York, p. 433.
Aubry, M.-P., 2015b. In: Aubry, M. (Ed.), Cenozoic Coccolithophores: Discoasterales (CC-E), New York. Micropaleontology Press. Atlas of Micropaleontology series, p. 532.
Aubry, M.-P., 2021. Coccolithophores: Cenozoic Discoasterales—Biology, Taxonomy, Stratigraphy, vol. 14. SEPM Society for Sedimentary Geology.
Backman, J., Raffi, I., Rio, D., Fornaciari, E., Pälike, H., 2012. Biozonation and biochronology of Miocene through Pleistocene calcareous nannofossils from low and middle latitudes. Newsl. Stratigr. 45, 221–244.
Bann, K.L., Tye, S.C., Maceachern, J.A., Fielding, C.R., Jones, B.G., 2008. Ichnological and sedimentological signatures of mixed wave- and storm-dominated deltaic deposits: examples from the Early Permian Sydney Basin, Australia. In: Hampson, G. J., Steel, R.J., Burgess, P.M., Dalrymple, R.W. (Eds.), Recent Advances in Models of Siliciclastic Shallow-Marine Stratigraphy, vol. 90. SEPM Society for Sedimentary Geology, pp. 293–332.
Bayet-Goll, A., Neto de Carvalho, C., 2020. Architectural evolution of a mixed-infuenced deltaic succession: lower-to-middle ordovician armorican quartzite in the southwest central iberian zone, penha garcia formation (Portugal). Int. J. Earth Sci. 109, 2495–2526.
Bermúdez, H.D., 2016. Esquema estratigráfico de secuencias del registro sedimentario del Cinturón Plegado de San Jacinto, Caribe colombiano. Extended abstract presented at the XII Simposio Bolivariano Exploración Petrolera en Cuencas Subandinas. Bogotá. September 26–28.
Bermúdez, H.D., Alvarán, M., Grajales, J.A., Restrepo, L., Rosero, J.S., Guzmán, C., Ruiz, E., Navarrete, R., Jaramillo, C., Osorno, F., 2009. Estratigrafía y evolución geológica de la secuencia sedimentaria del Cinturón Plegado de San Jacinto. XII Congreso Colombiano de Geología. Paipa, Colombia, pp. 1–28.
Bertling, M., Braddy, S., Bromley, R.G., Demathieu, G.D., Genise, J.F., Mikuláš, R., Nielsen, J.-K., Nielsen, K.S.S., Rindsberg, A.K., Schlirf, M., Uchman, A., 2006. Names for trace fossils: a uniform approach. Lethaia 39, 265–286.
Bhattacharya, J.P., 2006. Deltas. In: Posamentier, H.W., Walker, R.G. (Eds.), Facies Models Revisited, vol. 84. Society of Economic Paleontologists and Mineralogists Special Publication, pp. 237–292.
Bhattacharya, J.P., Giosan, L., 2003. Wave-influenced deltas: geomorphological implications for facies reconstruction. Sedimentology 50, 187–210.
Bhattacharya, J.P., MacEachern, J.A., 2009. Hyperpycnal rivers and prodeltaic shelves in the Cretaceous seaway of North America. J. Sediment. Res. 79, 184–209.
Birgenheier, L.P., Horton, B., McCauley, A.D., Johnson, C.L., Kennedy, A., 2017. A depositional model for offshore deposits of the lower Blue Gate Member, Mancos Shale, Uinta Basin, Utah, USA. Sedimentology 64, 1402–1438.
Boesiger, T.M., de Kaenel, E., Bergen, J.A., Browning, E., Blair, S.A., 2017. Oligocene to Pleistocene taxonomy and stratigraphy of the genus Helicosphaera and other placolith taxa in the circum North Atlantic Basin. J. Nannoplankt. Res. 37 (2–3), 145–175.
Bown, P., 1998. Calcareous Nannofossil Biostratigraphy. Chapman and Hall; Kluwer Academic.
Bridge, J.S., 2006. Fluvial facies models: recent developments. In: Posamentier, H.W., Walker, R.G. (Eds.), Facies Models Revisited, vol. 84. SEPM (Society for Sedimentary Geology), Special Publications, pp. 85–170.
Bromley, R.G., 1996. Trace Fossils: Biology, Taphonomy and Applications: London. Chapman & Hall, p. 361.
Buatois, L.A., Gingras, M.K., MacEachern, J.A., Mángano, M.G., Zonneveld, J.P., Pemberton, S.G., Netto, R.G., Martin, A.J., 2005. Colonization of Brackish–water systems through time. Evidence from the trace–fossil record. Palaios 20, 321–347.
Buatois, L.A., Saccavino, L.L., Zavala, C., 2011. Ichnologic signatures of hyperpycnal flow deposits in Cretaceous river–dominated deltas, Austral Basin, southern Argentina. In: Slatt, R.M., Zavala, C. (Eds.), Sediment Transfer from Shelf to Deep Water—Revisiting the Delivery System, AAPG Studies in Geology, vol. 61, pp. 153–170.
Buatois, L.A., Santiago, N., Herrera, M., Plink-Björklund, P., Steel, R.J., Espin, M., Parra, K., 2012. Sedimentological and ichnological signatures of changes in wave, river and tidal influence along a Neogene tropical deltaic shoreline. Sedimentology 59, 1568–1612.
Cattaneo, A., Steel, R.J., 2003. Transgressive deposits: a review of their variability. Earth Sci. Rev. 62 (3–4), 187–228.
Celis, S.A., Rodríguez-Tovar, F.J., Giraldo-Villegas, C.A., Pardo–Trujillo, A., 2021. Evolution of a fluvial-dominated delta during the Oligocene of the Colombian Caribbean: sedimentological and ichnological signatures in well-cores. J. S. Am. Earth Sci. 111, 103440.
Chalabe, A.C., Matrínez, M.A., Olivera, D.E., Canale, N., Ponce, J.J., 2022. Palynological analysis of sandy hyperpycnal deposits of the middle jurassic, lajas formation, neuquén basin, Argentina. J. S. Am. Earth Sci. 116, 103867.
Coates, L., MacEachern, J.A., 2007. The ichnological signatures of river- and wave-dominated delta complexes: differentiating deltaic and non-deltaic shallow marine successions, Lower Cretaceous Viking Formation and Upper Cretaceous Dunvegan Formation, West-Central Alberta. In: MacEachern, J.A., Bann, K.L., Gingras, M.K., Pemberton, S.G. (Eds.), *Applied Ichnology*. Society for Sedimentary Geology, Short Course Notes, vol. 52, pp. 227–255.
Cohen, K.M., Finney, S.C., Gibbard, P.L., Fan, J.-X., 2013. The ICS International Chronostratigraphic Chart: Episodes 36, 199–204.
Cole, G., Jerrett, R., Watkinson, M.P., 2021. A stratigraphic example of the architecture and evolution of shallow water mouth bars. Sedimentology 68, 1227–1254.
Collins, S.D., Johnson, H.D., Baldwin, C.T., 2019. Architecture and preservation in the fluvial to marine transition zone of a mixed–process humid–tropical delta: middle Miocene Lambir Formation, Baram Delta Province, north–west Borneo. Sedimentology 67, 1–46.
Collinson, J., Mountney, N., 2019. Sedimentary Structures –, fourth ed. Dunedin Academic Press Ltd, p. 340p.
Dalrymple, R.W., Choi, K., 2007. Morphologic and facies trends through the fluvial–marine transition in tide–dominated depositional systems: a schematic framework for environmental and sequence–stratigraphic interpretation. Earth Science Review 81, 135–174.
Dalrymple, R.W., Knight, R.J., Zaitlin, B.A., Middleton, G.V., 1990. Dynamics and facies model of a macrotidal sand–bar complex, cobequid bay—salmon river estuary (bay of fundy). Sedimentology 37, 577–612.
Dalrymple, R.W., Zaitlin, B.A., Boyd, R., 1992. Estuarine facies models: conceptual basis and stratigraphic implications. J. Sediment. Petrol. 62, 147–173.
Dalrymple, R.W., Baker, E.K., Harris, P.T., Hughes, M.G., 2003. Sedimentology and stratigraphy of a tide-dominated, foreland-basin delta (Fly river, Papua New Guinea). In: Sidi, F.H., Nummedal, D., Imbert, P., Darman, H., Posamentier, H.W. (Eds.), Tropical Deltas of Southeast Asia—Sedimentology, Stratigraphy, and Petroleum Geology, vol. 76. SEPM (Society for Sedimentary Geology), pp. 147–173.
Dalrymple, R.W., Kurcinka, C., Jablonski, B., Ichaso, A., Mackay, D., 2015. Deciphering the relative importance of fluvial and tidal processes in the fluvial–marine transition. In: Ashworth, P.J., Best, J.L., Parsons, D.R. (Eds.), *Fluvial–Tidal Sedimentology*. Developments in Sedimentology, vol. 68. Elsevier, pp. 3–45.
Dashtgard, S.E., La Croix, A.D., 2015. Sedimentological trends across the tidal–fluvial transition, Fraser River, Canada: a review and some broader implications. In: Ashworth, P.J., Best, J.L., Parsons, D.R. (Eds.), *Fluvial–Tidal Sedimentology*. Developments in Sedimentology, pp. 111–126.
D'Apolito, C., Jaramillo, C., Harrington, G., 2021. Miocene Palynology of the Solimões Formation (Well 1-AS-105-AM), Western Brazilian Amazonia. Smithsonian Contributions to Paleobiology. Smithsonian Institution Scholarly Press, Washington, D.C. No. 105.
Dashtgard, S.E., Gingras, M.K., MacEachern, J.A., 2009. Tidally modulated shorefaces. J. Sediment. Res. 79, 793–807.
Davidson-Arnott, R.G.D., Van Heyningen, A.G., 2003. Migration and sedimentology of longshore sandwaves, long point, lake erie, Canada. Sedimentology 50, 1123–1137.
Desjardins, P.R., Buatois, L.A., Mángano, M.G., 2012. Tidal flats and subtidal sand bodies. In: Knaust, D., Bromley, R.G. (Eds.), Trace Fossils as Indicators of Sedimentary Environments, Developments in Sedimentology, vol. 64, pp. 529–561.
Díez-Canseco, D., Buatois, L.A., Mángano, M.G., Rodriguez, W., Solorzano, E., 2015. The ichnology of the fluvial–tidal transition: interplay of ecologic and evolutionary controls. In: Ashworth, P.J., Best, J.L., Parsons, D.R. (Eds.), *Fluvial–Tidal Sedimentology*. Developments in Sedimentology. Elsevier, pp. 283–321.
Dueñas, H., 1980. Palynology of oligocene-miocene strata of borehole Q-E-22, planeta rica, northern Colombia. Review of paleobotany and palynology 30, 313–328.
Dueñas, H., 1983. Fluctuaciones del nivel del mar durante el depósito de los sedimentos basales de la Formación Ciénaga de Oro. Instituto nacional de investigaciones geológico mineras, INGEOMINAS. Bogotá, D.E. Revista de la academia colombiana de ciencias exactas. físicas y naturales XV, 58.
Dueñas, H., 1986. Geología y palinología de la Formación Ciénaga de Oro, Región Caribe Colombiana, vol. 18. Publicaciones Geológicas Especiales del Ingeominas, Bogotá, pp. 1–56.
Dueñas, H., Duque-Caro, H., 1981. Geología del Cuadrángulo F-8 (Planeta Rica). Bol. Geol. - Ingeominas 24 (1), 1–35 (Bogotá).
Duque-Caro, H., 1972. Ciclos tectónicos y sedimentarios en el Norte de Colombia y sus relaciones con la paleoecología. Bol. Geol. - Ingeominas 19, 1–23.
Duque-Caro, H., Guzmán Ospitia, G., Hernández, R., 1996. Geología de la plancha 38 Carmen de Bolívar, Escala 1:100.000. Instituto Colombiano de Geología y Minería INGEOMINAS, Bogotá, pp. 96–p.
Einsele, G., 2000. Sedimentary Basins. Evolution, Facies, and Sediment Budget. Second, Completely Revised and Enlarged, Edition. Springer, p. 795.
Enge, H.D., Howell, J.A., Buckley, S.J., 2010. The geometry and internal architecture of stream mouth bars in the Panther Tongue and the Ferron Sandstone Members, Utah, U.S.A. J. Sediment. Res. 80, 1018–1031.
Esperante, R., Rodríguez-Tovar, F.J., Nalin, R., 2021. Rhizoliths in Lower Pliocene alluvial fan deposits of the Sorbas Basin (Almería, SE Spain). Palaeogeogr. Palaeoclimatol. Palaeoecol. 567, 110281.
Flinch, J.F., 2003. Structural evolution of the Sinú-Lower Magdalena area (Northern Colombia). In: Bartolini, C., Buffler, R.T., Blickwede, J. (Eds.), The Circum-Gulf of Mexico and the Caribbean: Hydrocarbon Habitats Basin Formation, and Plate Tectonics, vol. 79. AAPG Memoir, pp. 776–796.
Frey, R.W., Pemberton, G.S., 1985. Biogenic structures in outcrops and cores. Approaches to ichnology. Bull. Can. Petrol. Geol. 33 (1), 72–115.
Gamero Diaz, H., Contreras, C., Lewis, N., Welsh, R., Zavala, C., 2011. Evidence of shelfal hyperpycnal deposition of Pliocene sandstones in the Oilbird Field, Southeast Coast, Trinidad: Impact on reservoir distribution. In: Slatt, R.M., Zavala, C. (Eds.), Sediment Transfer from Shelf to Deep Water-Revisiting the Delivery System, vol. 61. AAPG Stud. Geol., pp. 193–214
Gani, M.R., Bhattacharya, J.P., MacEachern, J.A., 2007. Using Ichnology to Determine the Relative Influence of Waves, Storms, Tides, and Rivers in Deltaic Deposits:

Examples from Cretaceous Western Interior Seaway, U.S.A. In: MacEachern, J.A., Bann, K.L., Gingras, M.K., Pemberton, S.G. (Eds.), *Applied Ichnology*. Society for Sedimentary Geology, Short Course Notes, vol. 52, pp. 209–225.
Geotec., 2003. Geología de los cinturones Sinú–San Jacinto. Plan 50 (51), 135, 59, 060, 61, 69, 70, 71, 79, 80. Bogotá. Geotec Ldta–Ingeominas.
Gerard, J.R.F., Bromley, R.G., 2008. Ichnofabrics in Clastic Sediments: Applications to Sedimentological Core Studies. Jean R.F. Gerard, Madrid, p. 97.
Gingras, M., MacEachern, J.A., 2012. Tidal Ichnology of Shallow–Water Clastic Settings. In: Davis, R.C., Dalrymple, R.W. (Eds.), Principles of Tidal Sedimentology, vol. 4, pp. 57–77.
Gingras, M.K., MacEachern, J.A., Pemberton, S.G., 1998. A comparative analysis of the ichnology of wave–and river–dominated allomembers of the Upper Cretaceous Dunvegan Formation. Bull. Can. Petrol. Geol. 46, 51–73.
Gingras, M.K., Pemberton, S.G., Saunders, T., Clifton, H.E., 1999. The ichnology of brackish water Pleistocene deposits at Willapa Bay, Washington: variability in estuarine settings. Palaios 14, 352–374.
Gingras, M.K., MacEachern, J.A., Dashtgard, S.E., 2011. Process ichnology and the elucidation of physico–chemical stress. Sediment. Geol. 237, 115–134.
Gómez, J., Montes, N.E., Nivia, Á., Diederix, H., 2015. Mapa Geológico de Colombia 2015. Bogotá. Ingeominas. Escala 1:1 000 000.
Gugliotta, M., Kurcinka, C.E., Dalrymple, R.W., Flint, S.S., Hodgson, D.M., 2016. Decoupling seasonal fluctuations in fluvial discharge from the tidal signature in ancient deltaic deposits: an example from the Neuquén Basin, Argentina. J. Geol. Soc. 173, 94–107.
Guzmán, G., 2007. Stratigraphy and Sedimentary Environment and Implications in the Plato Basin and the San Jacinto Belt Northwestern Colombia. Ph.D. Thesis. University of Liége, Belgium., p. 275
Guzmán, G., Gómez, E., Serrano, B.E., 2004. Geología de los cinturones del Sinú, San Jacinto y borde Occidental del Valle Inferior del Magdalena. Caribe Colombiano, vol. 24. Bogotá., p. 134. Escala 1:300.000.
Hansen, C.D., MacEachern, J.A., 2007. Application of the asymmetric delta model to along–strike facies variations in a mixed wave– and river–influenced delta lobe, Upper Cretaceous Basal Belly River Formation, central Alberta. In: MacEachern, J.A., Pemberton, S.G., Gingras, M.K., Bann, K.L. (Eds.), Applied Ichnology. Society for Sedimentary Geology, Tulsa, USA, pp. 256–272.
Hoorn, M.C., 1994. An environmental reconstruction of the palaeo-Amazon River system (Middle to Late Miocene, NW Amazonia). Palaeogeogr. Palaeoclimatol. Palaeoecol. 112, 187–238.
Howell, J.A., Skorstad, A., MacDonald, A., Fordham, A., Flint, S., Fjellvoll, B., Manzocchi, T., 2008. Sedimentological parameterization of shallow-marine reservoirs. Petrol. Geosci. 14, 17–34.
Hutchinson, D.K., Coxall, H.K., Lunt, D.J., Steinthorsdottir, M., de Boer, A.M., Baatsen, M., von der Heydt, A., Huber, M., Kennedy-Asser, A.T., Kunzmann, L., Ladant, J.-B., Lear, C.H., Moraweck, K., Pearson, P.N., Piga, E., Pound, M.J., Salzmann, U., Scher, H.D., Sijp, W.P., Śliwińska, K.K., Wilson, P.A., Zhang, Z., 2021. The Eocene–Oligocene transition: a review of marine and terrestrial proxy data, models and model–data comparisons. Clim. Past 17, 269–315.
Jaramillo, C., Ochoa, D., Contreras, L., Pagani, M., Carvajal-Ortiz, H., Pratt, L.M., Krishnan, S., Cardona, A., Romero, M., Quiroz, L., Rodriguez, G., Rueda, M., De la Parra, F., Moron, S., Green, W., Bayona, G., Montes, C., Quintero, O., Ramirez, R., Mora, A., Schouten, S., Bermudez, H., Navarrete, R.E., Parra, F., Alvaran, M., Osorno, J., Crowley, J.L., Valencia, V., Vervoort, J., 2010. Effects of Rapid Global Warming at the Paleocene-Eocene Boundary on Neotropical Vegetation. Science 330, 957–961.
Jaramillo, C.A., Rueda, M., Torres, V., 2011. A palynological zonation for the Cenozoic of the Llanos and Llanos Foothills of Colombia. Palynology 35, 46–84.
Johnson, S.M., Dashtgard, S.E., 2014. Inclined heterolithic stratification in a mixed tidal–fluvial channel: Differentiating tidal versus fluvial controls on sedimentation. Sediment. Geol. 301, 41–53.
Katz, M., Miller, E.K.G., Wright, J.D., Wade, B.S., Browning, J.V., Cramer, B.S., Rosenthal, Y., 2008. Stepwise transition from the Eocene greenhouse to the Oligocene icehouse. Nat. Geosci. 1, 329–334.
Knaust, D., 2017. Atlas of Trace Fossils in Well Core: Appearance, Taxonomy and Interpretation. Springer, Cham, Switzerland, p. 206.
Lamb, M.P., Mohrig, D., 2009. Do hyperpycnal-flow deposits record river-flood dynamics? *Geology*, GSA 37 (12), 1067–1070.
Lara, M., Salazar-Franco, A.M., Silva-Tamayo, J.C., 2018. Provenance of the Cenozoic siliciclastic intramontane Amagá Formation: Implications for the early Miocene collision between Central and South America. Sediment. Geol. 373, 147–162.
MacEachern, J.A., Bann, K.L., 2008. The role of ichnology in refining shallow marine facies models. In: Hampson, G.J., Steel, R.J., Burgess, P.M., Dalrymple, R.W. (Eds.), Recent Advances in Models of Siliciclastic Shallow-Marine Stratigraphy, vol. 90. SEPM Special Publication No, pp. 73–116.
MacEachern, J.A., Bann, K.L., 2020. The *Phycosiphon* Ichnofacies and the *Rosselia* Ichnofacies: Two new Seilacherian Ichnofacies for marine deltaic environments. J. Sediment. Res. 90, 855–886.
MacEachern, J.A., Stelck, C.R., Pemberton, S.G., 1999. Marine and marginal marine mudstone deposition: Paleoenvironmental interpretations based on the integration of ichnology, palynology and foraminiferal paleoecology. In: Bergman, K.M., Snedden, J.W. (Eds.), Isolated Shallow Marine Sand Bodies: Sequence Stratigraphic and Sedimentologic Interpretation, vol. 64. SEPM, Special Publication, pp. 205–225.
MacEachern, J.A., Bann, K., Bhattacharya, J.P., Howell, C.D., 2005. Ichnology of deltas: organism responses to the dynamic interplay of rivers, waves, storms and tides. In: Bhattacharya, B.P., Giosan, L. (Eds.), River Deltas: Concepts, Models and Examples, vol. 83. SEPM Special Publication, pp. 45–85.
MacEachern, J.A., Bann, K.L., Pemberton, S.G., Gingras, M.K., 2007a. The ichnofacies paradigm: high–resolution paleoenvironmental interpretation of the rock record. In: MacEachern, J.A., Bann, K.L., Gingras, M.K., Pemberton, S.G. (Eds.), *Applied Ichnology*. Society for Sedimentary Geology, Short Course Notes, vol. 52, pp. 27–64.
MacEachern, J.A., Pemberton, S.G., Gingras, M.K., Bann, K.L., Dafoe, L.T., 2007b. Use of trace fossils in genetic stratigraphy. In: Miller, W. (Ed.), Trace Fossils: Concepts, Problems, Prospects. Elsevier, pp. 110–134. III.
Manco-Garcés, A., Marín-Cerón, M.I., Sánchez-Plazas, C.J., Escobar-Arenas, L.C., Beltrán-Triviño, A., von Quadt, A., 2020. Provenance of the Ciénaga de Oro Formation: unveiling the tectonic evolution of the Colombian Caribbean margin during the Oligocene - Early Miocene. Bol. Geol. 42 (3), 205–226.
Mantilla-Pimiento, A., Jentzsch, G., Kley, J., Alfonso-Pava, C., 2009. Configuration of the Colombian Caribbean Margin: Constraints from 2D Seismic Reflection data and Potential Fields Interpretation. In: Lallemand, S., Funiciello, F. (Eds.), *Subduction Zone Geodynamics*, Frontier in Earth Sciences, pp. 247–272.
Martini, E., 1971. Standard Tertiary and Quaternary calcareous nannoplankton zonation. In: Farinacci, A. (Ed.), *Proceedings 2nd International Conference Planktonic Microfossils Roma*: Rome, vol. 2. Tecnosci., pp. 739–785
Martinius, A.W., Gowland, S., 2011. Tide-influenced fluvial bedforms and tidal bore deposits (Late Jurassic Lourinhã Formation, Lusitanian Basin, Western Portugal). Sedimentology 58, 285–324.
Maselli, V., Normandeau, A., Nones, M., Tesi, T., Langone, L., Trincardi, F., Bohacs, K.M., 2020. Tidal modulation of river–flood deposits: How low can you go? Geology 48, 663–667.
Makaske, B., 2001. Anastomosing rivers: a review of their classification, origin and sedimentary products. Earth Sci. Rev. 53 (3–4), 149–196.
Miall, A.D., 2014. Fluvial Depositional Systems. Springer Geology, p. 322.
Montes, C., Rodriguez-Corcho, A.F., Bayona, G., Hoyos, N., Zapata, S., Cardona, A., 2019. Continental margin response to multiple arc–continent collisions: The northern Andes–Caribbean margin. Earth Sci. Rev. 198, 102903.
Mora, J.A., Oncken, O., Le Breton, E., Ibánez-Mejia, M., Faccena, C., Veloza, G., Vélez, V., de Freitas, M., Mesa, A., 2017. Linking Late Cretaceous to Eocene tectonostratigraphy of the San Jacinto fold belt of NW Colombia with Caribbean plateau collision and flat subduction. Tectonics 36, 2599–2629.
Mora, J.A., Oncken, O., Le Breton, E., Mora, A., Veloza, G., Vélez, V., de Freitas, M., 2018. Controls on forearc basin formation and evolution: Insights from Oligocene to Recent tectonostratigraphy of the Lower Magdalena Valley basin of northwest Colombia. Mar. Petrol. Geol. 97, 288–310.
Mora-Bohórquez, J.A., Oncken, O., Le Breton, E., Ibánez-Mejia, M., Veloza, G., Mora, A., Vélez, V., de Freitas, M., 2020. Formation and Evolution of the Lower Magdalena Valley Basin and San Jacinto Fold Belt of Northwestern Colombia: Insights from Upper Cretaceous to Recent Tectono–Stratigraphy. In: Gómez, J., Mateus–Zabala, D. (Eds.), The Geology Of Colombia, Volume 3 Paleogene – Neogene. Servicio Geológico Colombiano, vol. 37. , Publicaciones Geológicas Especiales, pp. 21–66.
Mora-Páez, H., Kellogg, J.N., Freymueller, J., Mencin, D., Fernandes, R.M.S., Diederix, H., LaFemina, P., Cardona-Piedrahita, L., Lizarazo, S., Peláez-Gaviria, J.-R., Díaz-Mila, F., Bohórquez-Orozco, O., Giraldo-Londoño, L., Corchuelo-Cuervo, Y., 2019. Crustal deformation in the northern Andes – A new GPS velocity field. J. S. Am. Earth Sci. 89, 76–91.
Mount, J., 1985. Mixed siliciclastic and carbonate sediments: a proposed first-order textural and compositional classification. Sedimentology 32, 435–442.
Moyano-Paz, D., Richiano, S., Varela, A.N., Gómez Decál, A.R., Poiré, D.G., 2020. Ichnological signatures from wave– and fluvial–dominated deltas: The La Anita Formation, Upper Cretaceous, Austral–Magallanes Basin, Patagonia. Mar. Petrol. Geol. 114, 104168.
Moyano-Paz, D., Isla, M.F., MacEachern, J.A., Richiano, S., Gómez-Dacal, A.R., Varela, A. N., Poiré, D.G., 2022. Evolution of an aggradational wave-dominated delta: Sediment balance and animal-substrate dynamics (Upper cretaceous La Anita Formation, Southern Patagonia). Sediment. Geol., 106193
Mulder, T., Syvitski, J.P.M., Migeon, S., Faugères, J.C., Savoye, B., 2003. Marine hyperpycnal flows: initiation, behavior and related deposits: a review. Mar. Petrol. Geol. 20, 861–882.
Mutti, E., Tinterri, R., Benevelli, G., di Biase, D., Cavanna, G., 2003. Deltaic, mixed and turbidite sedimentation of ancient foreland basins. Mar. Petrol. Geol. 20 (6–8), 733–755.
Nagy, J., 1992. Environmental significance of foraminiferal morphogroups in Jurassic North sea deltas. Palaeogeogr. Palaeoclimatol. Palaeoecol. 95, 111–134.
Nichols, G., 2009. Sedimentology and Stratigraphy. Blackwell Publishing, A John Wiley and Sons, Ltd., Publication, p. 432.
Noda, A., 2016. Forearc basins: Types, geometries, and relationships to subduction zone dynamics. Geol. Soc. Am. Bull. 128 (5–6), 879–895.
Olariu, C., Bhattacharya, J.P., 2006. Terminal distributary channels and delta front architecture of river-dominated delta systems. J. Sediment. Res. 76 (2), 212–233.
Osorio-Granada, E., Pardo-Trujillo, A., Restrepo-Moreno, S.A., Gallego, F., Muñoz, J., Plata, A., Trejos-Tamayo, R., Vallejo, F., Barbosa-Espitia, A., Cardona-Sánchez, F.J., Foster, D.A., Kamenov, G., 2020. Provenance of Eocene-Oligocene sediments in the San Jacinto Fold Belt: Paleogeographic and geodynamic implications for the northern Andes and the southern Caribbean. Geosphere 16 (1), 210–228.
Pardo-Trujillo, A., Cardona, A., Giraldo, S.A., León, S., Vallejo, D.F., Trejos-Tamayo, R., Plata, A., Ceballos, J., Echeverri, S., Barbosa-Espitia, A., Slattery, J., Salazar-Ríos, A., Botello, G.E., Celis, S.A., Osorio-Granada, E., Giraldo-Villegas, C.A., 2020. Sedimentary record of the Cretaceous–Paleocene arc–continent collision in the northwestern Colombian Andes: insights from stratigraphic and provenance constraints. Sediment. Geol. 401, 105627.
Pardo-Trujillo, A., Jaramillo, C., 2014. Palinología y paleoambientes de los depósitos paleógenos del sector central de la Cordillera Oriental Colombiana: 35 millones de

años de historia de la vegetación neotropical. In: Rangel, J.O. (Ed.), Colombia Diversidad Biótica XIV: La región de la Orinoquía de Colombia. Edition 1. Palinología y paleoambientes. Universidad Nacional.
Pearson, D.L., 1984. Pollen/spore Colour 'standard. Version #2. Phillips Petroleum Company Exploration Projects Section (privately distributed. Bartlesville, Oklahoma [privately distributed]).
Pemberton, S.G., Wightman, D.M., 1992. Ichnological characteristics of brackish water deposits. In: Pemberton, S.G. (Ed.), *Applications Of Ichnology To Petroleum Exploration*. A Core Workshop: SEPM, vol. 17, pp. 141–167.
Pemberton, S.G., MacEachern, J.A., Ranger, M.J., 1992. Ichnology and event stratigraphy: the use of trace fossils in recognizing tempestites. In: Pemberton, S.G. (Ed.), Applications of Ichnology to Petroleum Exploration. A Core Workshop, vol. 17. SEPM Core Workshop, pp. 85–117.
Pemberton, S.G., MacEachern, J.A., Saunders, T., 2004. Stratigraphic applications of substrate specific ichnofacies: delineating discontinuities in the rock record. In: McIlroy, D. (Ed.), The Application of Ichnology to Palaeoenvironmental and Stratigraphic Analysis, vol. 228. Geological Society, Special Publications, p. 2962.
Perch-Nielsen, K., 1985. Cenozoic calcareous nannofossils. In: Bolli, H.M., Saunders, J.B., Perch-Nielsen, K. (Eds.), Plankton Stratigraphy. Cambridge University Press, Cambridge, pp. 427–554.
Raigosa, M., 2018. Caracterización estratigráfica, microfacial y diagenética de las formaciones Toluviejo y El Floral en la región onshore del Cinturón Plegado SinúSan Jacinto. Servicio Geológico Colombiano, Bogotá, p. 119.
Reading, H.G., 1996. Sedimentary Environments: Processes, Facies and Stratigraphy, third ed. Blackwell Publishing company, Oxford, p. 688p.
Retallack, G.J., 2001. Soils of the Past: an Introduction to Paleopedology. Blackwell Science, Oxford, p. 549.
Romito, S., Mann, P., 2020. Tectonic terranes underlying the present-day Caribbean plate: their tectonic origin, sedimentary thickness, subsidence histories and regional controls on hydrocarbon resources. In: Davison, I., Hull, J.N.F., Pindell, J. (Eds.), Geological Society, London, Special Publications vol. 504, 343, 1, The Basins, Orogens and Evolution of the Southern Gulf of Mexico and Northern Caribbean.
Rossi, V.M., Steel, R., 2016. The role of tidal, wave and river currents in the evolution of mixed-energy deltas: Example from the Lajas Formation (Argentina). Sedimentology 63, 824–864.
Rossi, V.M., Perillo, M.M., Steel, R.J., Olariu, C., 2017. Quantifying mixed-process variability in shallow-marine depositional systems: what are sedimentary structures really telling us? J. Sediment. Res. 87, 1060–1074.
Salazar-Ortiz, E.A., Rincón-Martínez, D., Páez, L.-A., Restrepo, S.M., Barragán, S., 2020. Middle Eocene mixed carbonate-siliciclastic systems in the southern Caribbean (NW colombian margin). J. S. Am. Earth Sci. 99, 102507.
Savrda, C.E., Ozalas, K., Demko, T.H., Hichison, R.A., Scheiwe, T.D., 1993. Log–grounds and the ichnofossil *Teredolites* in transgressive deposits of the Clayton Formation (Lower Paleocene), Western Alabama. Palaios 8, 311–324.
Schultz, S.K., MacEachern, J.A., Catuneanu, O., Dashtgard, S., 2020. Coeval deposition of transgressive and normal regressive stratal packages in a structurally controlled area of the Viking Formation, central Alberta, Canada. Sedimentology 67 (6), 2974–3002.
Selley, R.C., 1985. The Reservoir, Elements of Petroleum Geology. W. H. Freeman and Company, New York, pp. 219–275.
SGC, 2019. Memoria explicativa de la plancha 81 – Puerto Libertador a escala 1:100000. Departamento de Córdoba. Servicio Geológico Colombiano, p. 220.
Shanmugam, G., 2009. Slides, slumps, debris flows, and turbidity currents. In: Steele, J. H., Thorpe, S.A., Turekian, K.K. (Eds.), Encyclopedia of Ocean Sciences, second ed. Academic Press (Elsevier), Waltham, MA, pp. 447–467.
Shanmugam, G., 2021. Gravity flows: debris flows, grain flows, liquefied/fluidized flows, turbidity currents, hyperpycnal flows, and contour currents. In: Shnmugan, G. (Ed.), *Mass Transport, Gravity Flows, and Bottom Currents*. Downslope and Alongslope Processes and Deposits. Academic Press (Elsevier), Waltham, pp. 89–148 (Chapter 3).
Shchepetkina, A., Gingras, M.K., Mángano, M.G., Buatois, L.A., 2019. Fluvio–tidal transition zone: Terminology, sedimentological and ichnological characteristics, and significance. Earth Sci. Rev. 192, 214–235.
Silva-Tamayo, J.C., Sierra, G., Correa, L., 2008. Tectonic and climate driven fluctuations in the stratigraphic base level of a Cenozoic continental coal basin, northwestern Andes. J. S. Am. Earth Sci. 26–4, 369–382.
Silva-Arias, A., Páez-Acuña, L.A., Rincón-Martínez, D., Tamara-Guevara, J.A., Gomez-Gutierrez, P.D., López-Ramos, E., Restrepo-Acevedo, S.M., Mantilla-Figueroa, L.-C., Valencia, V., 2016. Basement characteristics in the Lower Magdalena Valley and the Sinú and San Jacinto Fold Belts: evidence of a Late Cretaceous magmatic arc at the South of the Colombian Caribbean. Ciencia, Tecnología y Futuro 6, 5–36.
Silva-Tamayo, J.C., Lara, M., Salazar-Franco, A.M., 2020. Oligocene – Miocene coal–bearing successions of the Amagá Formation, Antioquia, Colombia: Sedimentary environments, stratigraphy, and tectonic implications. In: Gómez, J., Mateus–Zabala, D. (Eds.), The Geology of Colombia, Volume 3 Paleogene – Neogene. Servicio Geológico Colombiano, vol. 37. , Publicaciones Geológicas Especiales, Bogotá, p. 23.
Simmons, M.D., Miller, K.G., Ray, D.C., Davies, A., van Buchem, F.S.P., Gréselle, B., 2020. Phanerozoic Eustasy. In: Gradstein, F., Ogg, J.G., Schmitz, M.D., Ogg, G.M. (Eds.), Geologic Time Scale 2020, pp. 357–400 (Chapter 13).
Slater, S.M., McKie, T., Vieira, M., Wellman, C.H., Vajda, V., 2017. Episodic river flooding events revealed by palynological assemblages in Jurassic deposits of the Brent Group, North Sea. Palaeogeogr. Palaeoclimatol. Palaeoecol. 485, 389–400.
Talling, P.J., Masson, D.G., Sumner, E.J., Malgestini, G., 2012. Subaqueous sediment density flows: depositional processes and deposit types. Sedimentology 59, 1937–2003.
Taylor, A.M., Goldring, R., 1993. Description and analysis of bioturbation and ichnofabric. Journal of the Geological Society of London 150, 141–148.
Thomas, F.C., Murney, M.G., 1985. Techniques for extraction of foraminifers and ostracodes from sediment samples. Can. Tech. Rep. Hydrogr. Ocean Sci. 54, 24.
Traverse, A., 2007. Paleopalynology, , second ed.vol. 28. Springer, Topics in Geobiology, Dordrecht, p. 813.
van Yperen, A.E., Holbrook, J.M., Poyatos-Moré, M., Midtkandal, I., 2019. Coalesced delta front sheet-like sandstone bodies from highly avulsive distributary channels: the low-accommodation Mesa Rica Sandstone (Dakota Group, New Mexico, USA). J. Sediment. Res. 89, 654–678.
Wade, B.S., Pearson, P.N., Berggren, W.A., Pälike, H., 2011. Review and revision of Cenozoic tropical planktonic foraminiferal biostratigraphy and calibration to the geomagnetic polarity and astronomical time scale. Earth Sci. Rev. 104, 111–142.
Wade, B.S., Olsson, R.K., Pearson, P.N., Huber, B.T., Berggren, W.A., 2018. Atlas of Oligocene Planktonic Foraminifera, vol. 46. Cushman Foundation for Foraminiferal Research, Special Publication, pp. 1–524.
Warne, A.G., Meade, R.H., White, W.A., Guevara, E.H., Gibeaut, J., Smyth, R.C., Aslan, A., Tremblay, T., 2002. Regional controls on geomorphology, hydrology, and ecosystem integrity in the Orinoco Delta, Venezeula. Geomorphology 44, 273–307.
Wei, X., Steel, R.J., Ravnas, R., Jiang, Z., Olariu, C., Li, Z., 2016. Variability of tidal signals in the Brent Delta Front: New observations on the Rannoch Formation, northern North Sea. Sediment. Geol. 335, 166–179.
Wentworth, C.K., 1922. A Scale of Grade and Class Terms for Clastic Sediments. J. Geol. 30, 377–392.
Wilford, D.J., Sakals, M.E., Innes, J.K., Sidle, R.C., 2005. Fans with forests: contemporany hydrogeomorphic processes on fans with forests in west central British Columbia, Canada. In: Harvey, A.M., Mather, A.E., Stokes, M. (Eds.), Alluvial Fans: Geomorphology, Sedimentology, Dynamics. Geological Society, London, Special Publications, pp. 25–40.
Yang, B.C., Dalrymple, R.W., Chun, S.S., 2005. Sedimentation on a wave dominated, open–coast tidal flat, south–western Korea: a summer tidal flat–winter shoreface. Sedimentology 52, 235–252.
Young, J.R., 1998. Neogene. In: Bown, P.R. (Ed.), Calcareous Nannofossil Biostratigraphy. British Micropalaeontological Society Publication Series, pp. 225–265.
Young, J.R., Geisen, M., Cros, L., Kleijne, A., Sprengel, C., Probert, I., Østergaard, J., 2003. A guide to extant coccolithophore taxonomy. J. Nannoplankt. Res. 1, 1–125.
Young, J.R., Bown, P.R., Lees, J.A., 2017. Nannotax3 Website. International Nannoplankton Association: International Nannoplankton Association. http://www.mikrotax.org/Nannotax3.
Zapata, S., Patiño, A., Cardona, A., Parra, M., Valencia, V., Reiners, P., Oboh-Ikuenobe, F., Genezini, F., 2020. Bedrock and detrital zircon thermochronology to unravel exhumation histories of accreted tectonic blocks: An example from the Western Colombian Andes. J. S. Am. Earth Sci. 103, 102715.
Zavala, C., 2020. Hyperpycnal (over density) flows and deposits. J. Palaeogeogr. 9, 17.
Zavala, C., Pan, S.X., 2018. Hyperpycnal flows and hyperpycnites: Origin and distinctive characteristics. Lithologic Reservoirs 3 (1), 1–27.
Zavala, C., Arcuri, M., Di Meglio, M., Gamero Diaz, H., Contreras, C., 2011. A genetic facies tract for the analysis of sustained hyperpycnal flow deposits. In: Slatt, R.M., Zavala, C. (Eds.), Sediment Transfer from Shelf to Deep Water Revisiting the Delivery System, AAPG Studies in Geology, vol. 61, pp. 31–51.
Zavala, C., Arcuri, M., Blanco Valiente, L., 2012. The importance of plant remains as a diagnostic criteria for the recognition of ancient hyperpycnites. Rev. Paléobiol. 11, 457–469.
Zavala, C., Arcuri, M., Di Meglio, M., Zorzano, A., Goitia Antezana, V.H., Arnez Espinosa, L.R., 2016. Prodelta Hyperpycnites: Facies, Processes and Reservoir Significance. Examples from the Lower Cretaceous of Russia. International Conference and Exhibition. SEG Global Meeting, Barcelona, Spain, p. 73.